A KIRKWOOD-BUFF FORCE FIELD FOR POLYOXOANIONS IN WATER

by

JIN ZOU

B.E., Nanjing University of Sci. & Tech., China, 2007

A Thesis

submitted in partial fulfillment of the requirements for the degree

MASTER OF SCIENCE

Department of Chemistry
College of Arts and Sciences

KANSAS STATE UNIVERSITY
Manhattan, Kansas

2010

Approved by:

Major Professor
Dr. Paul E. Smith

Copyright

Abstract

The increasing importance of ion-water interactions in the field of chemistry and biology is leading us to examine the structure and dynamic properties of molecules of interest, based on the application of computer-aided models using molecular dynamics simulations. To enable this type of MD study, a molecular mechanics force field was developed and implemented. Kirkwood-Buff theory has been proved to be a powerful tool to provide a link between molecular quantities and corresponding thermodynamic properties. Parameters are the vital basis of a force field. KB integrals and densities were used to guide the development of parameters which could describe the activity of aqueous solutions of interest accurately. In this work, a Kirkwood-Buff Force Field (KBFF) for MD simulation of ammonium sulfate, sodium sulfate, sodium perchlorate and sodium nitrate are presented. Comparison between the KBFF models and existing force fields for ammonium sulfate was also performed and proved that KBFF is very promising. Not only were the experimentally observed KB integrals and density reproduced by KBFF, but other properties like self diffusion constant and relative permittivity are also well produced.

Table of Contents

List of Figures

List of Tables

Acknowledgements

This thesis arose out of my research which started when I came to Dr. Smith's group more than two years ago. It is a pleasure to work with those amazing people in this department who help me in assorted ways and convey my gratitude to them.

First of all, I want to thank my advisor Dr. Paul E. Smith, a productive chemist with contagious enthusiasm and joy, a persuasive instructor with skill and patience. It has been an honor to be his student. I appreciate all his time and ideas to make my M.S. experience meaningful. I am indebted to him more than he knows.

The members of the Smith group give so many contributions both on personal and professional time at KSU. Many thanks go to them. The group has been a source of friendships as well as good advice and collaboration. I am especially grateful for Moon Bae Gee who is always a source of valuable advice in my research and grants me his time for teaching. Additionally, the beautiful view in Manhattan is keeping me in good spirits and wonderful friends here make it more than a temporary place of study.

I gratefully thank Dr. Stefan Bossmann and Dr. Christine Aikens for their acceptance to be my committee members, their precious time to read and give me constructive comments on this thesis.

Lastly, I would like to thank my parents for all their love, unconditional support and encouragement to pursue my interests. It is them that make me always believe I can fly.

Dedication

To my parents

CHAPTER 1 - Introduction

1.1 Molecular Simulation

1.1.1 General Introduction

Molecular simulation is a very popular computing method due to a rapid advance of computer power during the past several decades. Not only does it give us the simplified and idealized description of a molecule with a three-dimensional representation of structure at the atomic level, but also it allows us to mimic the behavior of molecules and molecular systems in order to determine macroscopic properties. We can verify the accuracy of the model by comparing simulation results with experimental data. Given sufficient computing time, discrepancies can be attributable to a failure of the model to represent molecular behavior. It is also a very useful tool for testing a model. In addition, we can use a given model system to evaluate a theory by comparing the results from a simulation of that given model system with predictions of a particular theory applied to that same model.[1-3]

At the same time, advances in measurement devices, like atomic force microscopy (AFM),[4] allow us to image, measure physical and biological phenomena occurring at the microscopic level, giving us more data to test the accuracy of our model by comparing. However, even though experimentalists can provide detailed information of biomolecules from state-of-the-art modern technology, like AFM, it is still difficult to study directly how these individual biomolecules move and function on short time scales. Simulations play a central role in filling in these crucial gaps. What is more, many current research ideas involve large-scale experimentation but the prohibitive cost of the necessary experiments simply makes it impracticable, while computer simulation can work as a substitute. When it comes to

environmental issues, some chemical experiments involve serious pollution and toxicity issues, while molecular simulation is capable of yielding useful information in an environmentally friendly way.[5-6] Experimentalists cast some doubt on the validity of molecular modeling even today. However, in the past, molecular simulation has already shown its validity and practical worth in the study of the structure and function of molecules.[7-8] This is a rapidly growing area with a myriad of exciting opportunities.

The history of computer simulations bears a remarkable resemblance to modern computers, since computational power was combined with theoretical and algorithmic developments based on the concepts of statistical mechanics (SM) introduced by Ludwig Boltzmann(1844-1906) and Josiah Willard Gibbs(1839-1903).[9] Computer simulation developed to an increasing range and depth based on the application of statistical mechanics.[10,11] SM is aimed at studying macroscopic systems from a molecular point of view. The connection between microscopic molecular details and observable macroscopic properties such as energy, heat capacity, pressure, volume or entropy is made by SM based on quantum mechanics which provides the fundamental details for calculating the intermolecular interactions.[12] SM takes advantage of rigorous statistical functions to deduce the behavior of the whole systems containing a large number of individual molecules. We construct an ensemble consisting of a large number of systems to apply statistical theory to the system of interest. There exist different ensembles with different characteristics. Each ensemble has a different microstate, but all of the microstates share the same macrostate. The common ensembles we use are microcanonical ensemble (NVE), canonical ensemble (NVT), grand canonical ensemble (μ, V, T) and isobaric-isothermal ensemble (NPT). Microcanonical, canonical and isobaric-isothermal ensemble are closed systems because the number of particles in each microstate is constant. In the grand

canonical ensemble, the passage of molecules between each other is allowed through a permeable wall, so it is an open ensemble. In statistical mechanics, ensemble averages corresponding to one certain experimental observable are taken over all of the systems in this ensemble simultaneously.[13]

1.1.2 Molecular Dynamics Simulation

Today, molecular simulation is increasingly providing valuable insights into macroscopic properties and microscopic details. However, there are still limitations in time scale and system size due to high computational cost.[14] Molecular simulation, including Monte Carlo (MC)[15] and Molecular dynamics (MD)[16] computing methods are now two of the most powerful tools that are used to explore the statistical mechanics of chemical systems or larger systems. Molecular Dynamics simulation is an important technique for researchers to compute the equilibrium and transport properties of a many-body system. From a number of pioneering studies, it had its modest beginnings in the late 1950s when Alder and Wainwright first introduced the molecular dynamics method.[17] In 1964, the first simulation was performed by Rahman using a realistic potential for liquid argon.[18,19] In traditional MD simulations, the particles move in a simulation cell and obey the laws of classical mechanics based on Newton's equations of motion. The instantaneous forces acting on the particles are calculated from potential energy functions.[20-23] In contrast to the Monte Carlo method which relies on transition probabilities, molecular dynamics solves the equations of motion of the molecules to generate new configurations.[24-26] Only MD can be used to obtain time-dependent properties of the system, like the viscosity coefficient, because MD includes time explicitly. The challenges are great

considering computers have limited power and capacity and suitable algorithms have to be developed.[27]

Figure 1. 1 A brief overview of how a molecular dynamics simulation is performed

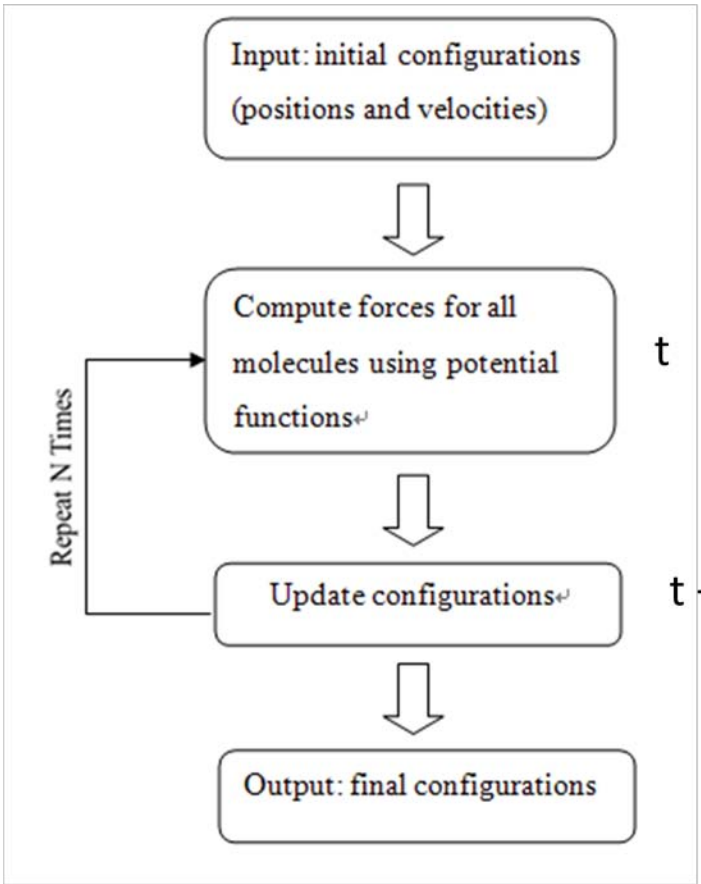

A parallel set of developments took place for the Monte Carlo method, which was introduced in a seminal paper by Metropolis et at in 1953.[28] It involves a stochastic strategy that relies on probabilities. It is a comparatively simple simulation and applicable for μ VT ensemble because it can be used for simulation with varying particle numbers, while this is difficult in MD. In the Monte Carlo process, a new configuration is obtained typically by displacing, exchanging, removing or adding a molecule. The acceptance of a new configuration is dependent on the Boltzmann distribution, that is to say the new configurations are generated with probability ∝

$e^{-\beta E}$ in the NVT ensemble. If the attempted change is rejected, then the old state is counted as the new state.[29-32] Normally, the new state will be accepted with high probability if it has a lower energy. Monte Carlo simulation does not provide time information, so it cannot determine dynamic properties, like transport properties. And when it comes to collective chain motions, MD performs better than MC approaches.

In short, Monte Carlo (MC) simulation provides ensemble averages, while Molecular Dynamics (MD) simulation provides time averages (ergodic hypothesis).[33,34]

1.2 Force Fields

The history of force fields started with simple harmonic force fields. From 1970, two classes of force field were gradually developed. One was for molecules with less than 100 atoms; the other was for macromolecules.[35,36] Now we have different force fields for different purposes. Not only do we have the highly accurate force fields allowing for more accurately calculated energies with increased speed specifically designed for small molecules,[37] but also we have successfully developed simpler more efficient force fields for studying large biomolecular systems. The commonly used biomolecular force field includes AMBER,[38] CHARMM,[39] OPLS[40] and GROMOS.[41] Generally, the relationship between chemical structure and energy is made by the application of mathematical equations. In addition, proper parameters must be developed for these mathematical equations, because we cannot get any useful information about structure-energy relationship if there are only mathematical equations available. In combination, the set of empirical equations and fitted parameters comprise a force field. We can apply the same mathematical equation to different chemical systems by using different parameters. Therefore, it is critical to define the parameters properly in order to obtain a correct description

of the system. In the molecular mechanics model, a molecule is described as a series of simple spheres (atoms) linked by springs (bonds). A simple force-field normally describes the bonded interactions using bond lengths, bond angles, torsions and the nonbonded interactions including Van der Waals and electrostatic interactions between atoms that are not directly bonded.[42-48] The observables that can be used to parameterize a force field are mostly obtained from experimental data. For instance, the structural parameters like bond length and angle can be obtained from X-ray or neutron diffraction studies on crystals or from spectroscopic measurements in liquids or gas phase.

Choosing a correct force field depends on the accuracy needed for the intended purpose. For example, when the intermolecular interactions are more significant than intramolecular interactions, a united-atom force field is a better option than all-atom force field to simulate molecular systems. All-atom force fields, as the name suggests, represent all the atoms in the system. United-atom force fields, on the other side, do not include an explicit representation of relatively unimportant atoms like nonpolar hydrogens. For example, methyl group in united-atom force field is simply treated as a single interaction center.[49,50] Usually we enlarge the van der Waals radius to increase the size of the atoms they are bonded to. This method can be taken further to deal with larger functional groups.[51] There is no doubt that neglecting some certain unimportant atoms will lead to a poorer accuracy, but it can provide a large saving in computer time and can satisfy the intended need if the inaccuracy is not too high.[52-55]

The total energy of the system is described as below,

$$E_{total} = E_{bonded} + E_{nonbonded} \quad (1.1)$$

within the molecular framework, the total energy is described in terms of a sum of contributions from bonded terms and nonbonded terms to describe the behavior of different kinds of atoms and bonds.

1.2.1 Bonded Interactions

The bonded terms include bond stretching, angle bending and torsion terms so that,[56,57]

$$E_{bonded} = E_{bond} + E_{angle} + E_{torsion} \quad (1.2)$$

- Bond stretching is represented by a simple harmonic function.[58] In molecular mechanics simulations, the displacement of the bond length from equilibrium is usually so small that it can be approximated to undergo simple harmonic motion.

$$E_{bond} = \sum_{bonds} \frac{1}{2} k_r (r - r_0)^2 \quad (1.3)$$

where k_r is the stretching force constant, r_o is the equilibrium bond distance, and r is the bond distance.

- Angle bending is represented by a simple harmonic function, obeying Hooke's law.[59]

$$E_{angle} = \sum_{angles} \frac{1}{2} k_\theta (\theta - \theta_0)^2 \quad (1.4)$$

where k_θ the bending is force constant, θ_0 is the equilibrium valence angle, and θ is the valence angle.

- The torsional contributions consist of proper dihedral and improper dihedral.[60-61] The proper dihedral term is modeled by a simple periodic function. The improper torsion is not a regular torsion angle but it is often necessary to restrict out-of-plane bending motion,

such as keeping planar groups in one plane or to maintaining their original chirality by preventing molecules from flipping over to their mirror images. The potentials are commonly given by,

$$E_{torsion} = \sum_{torsions} \frac{V_n}{2}[1 + \cos(n\varphi - \delta)] \quad (1.5)$$

$$E_{improper} = \sum_{improper} \frac{k_w}{2}(\omega - \omega_0)^2 \quad (1.6)$$

where V_n is force constant, n is periodicity of the angle which determines how many peaks and wells in the potential, δ is phase of the angle, k_w is force constant, ω is the torsion angle, and ω_0 is the equilibrium torsion angle.

1.2.2 Nonbonded Interactions

The nonbonded terms typically include van der Waals and electrostatic terms between pairs of atoms separated by three or more bonds,

$$E_{nonbonded} = E_{vanderwaals} + E_{electrostatic} \quad (1.7)$$

- The van der Waals term describes the interaction between two uncharged molecules or atoms, arising from a balance between repulsive and attractive forces.[62-64] Repulsion and attraction is almost equal to zero and cancel out each other if the separation between two atoms is infinite, but the repulsion gradually dominates once the separation is small. This provides the optimal separations between any two atoms i and j for which the systems is the most stable.

$$E_{vanderwaals} = \sum_{i<j} 4\varepsilon_{ij}\left[\frac{\sigma_{ij}^{12}}{r_{ij}^{12}} - \frac{\sigma_{ij}^{6}}{r_{ij}^{6}}\right] \quad (1.8)$$

where different combination rules are applied, $\varepsilon_{ij} = \sqrt{\varepsilon_i \varepsilon_j}, \sigma_{ij} = \frac{1}{2}(\sigma_i + \sigma_j)$ *or* $\sigma_{ij} = \sqrt{\sigma_i \sigma_j}$; ε_{ij} is the depth of potential well, σ_{ij} is the finite distance at which inter-particle potential is zero, and r_{ij} is the distance between two particles. In our work, the geometric average is used to determine both ε_{ij} and σ_{ij} . The r^{-12} term describes the short range repulsive potential; while the r^{-6} term describes the long range attractive potential.

- The electrostatic term involves a simple Coulombic expression describing the interactions between two point charges.[65,66] It can be either attractive or repulsive according to,

$$E_{electrostatic} = \frac{1}{4\pi\varepsilon_o} \sum_{i<j} \frac{q_i q_j}{r_{ij}} \tag{1.9}$$

where r_{ij} is the distance between two ions, q is the partial charge on each atom, and ε_o is electrical permittivity of free space. We can obtain an initial guess at the atomic charges (q) using results from ab initio calculations together with a population analysis or a fit to the electrostatic potential outside the molecule.[67] In quantum calculations, the atomic point charges are tailored to approximate the electrostatic field outside the molecule. In an empirical force field, they are effective condensed phase parameters to model long-range interactions. The transfer of charges between the two techniques is thus often unreliable. A better transferability is obtained if the quantum mechanical calculation includes a reaction field correction to mimic bulk solvent, and the derived charges are constrained to reproduce the effective dipole moment of the molecule in solution.[68-72]

In the potential energy calculation non-bonded interactions are the most time consuming part of a molecular dynamics simulation. The non-bonded terms are computed between each atom and every other atom. Normally, it may take approximately 99% of the time of the total

energy calculation. So it is very necessary to improve the non-bonded calculations. Periodic Boundary Conditions (PBC) simplifies the calculation of interactions. PBC only uses a small number of particles to simulate a large bulk solution. The central box is surrounded by 26 neighbors in the view of 3-D dimension. Those replica boxes are related to the central box by simple translations. Forces on the particles in central box are calculated from particles within the central box as well as in the neighboring boxes.[73]

Non-bonded interactions decrease as distance increases. The Coulombic interaction is a summation of all charge–charge interactions. They are slowly converging and therefore a large computational burden. Therefore, terminating the interaction between two atoms beyond a certain distance is necessary to speed up the computation. Molecular forces can be divided into two classes: short-range or long-range interactions. Different techniques are required to deal with different needs. We impose a cut-off distance, which is often less than a half the length of the simulation box, to the short-range interaction. The long-range interaction is then defined as the one beyond the cut-off distance. Usually, the potential is set to zero beyond cut-off distance. Simply increasing the cutoff distance to be sufficiently large can raise the computational cost, even if it increases the accuracy.[74-76] An alternative to deal with this problem is to calculate long-range interaction by special methods such as Ewald Sums.[77] Ewald Sums have proven to give satisfactory results with reasonable computer times. This method splits the potential into two parts, one of which is a short-range term calculated directly in real space, and the other of which is long-range term calculated in Fourier or reciprocal space. With the advent of increased computer power and new algorithms for efficient calculating long-range interactions, a simple cut-off treatment of long-range interaction is not necessary any more. Fortunately, Particle-Mesh

Ewald (PME) and Particle-Particle Particle-Mesh Methods (PPPM) have been developed recently to improve the performance of the reciprocal sum.[78,79]

1.2.3 Development of Force Fields

There are, of course, important limitations to the simple molecular mechanics representation. Our concerns about developing existing force field mostly focus on two areas. The first is accuracy. We oversimplify electrostatic interactions by including a point charge on each atom. This simple representation obviously cannot incorporate the full electrostatic properties (like multipole moments) of a molecule. Most current force fields use a "fixed-charge" model by which each atom is assigned a single value for the atomic charge that is not affected by the local electrostatic environment. Development of next-generation force fields have incorporated models for polarizability, in which a particle's charge is influenced by electrostatic interactions with its neighbors.[75-80] For example, polarizability can be approximated by the introduction of induced dipoles. Although polarizable force fields have been quite successful in modeling a wide variety of molecular systems, the common use has been inhibited by the high computational expense associated with calculating the local electrostatic field.[81-86]

The second focus is efficiency. The computational approaches that are currently available can be broadly divided into implicit and explicit solvation models. In the explicit solvent approach, water molecules are treated as discrete individuals necessitating a detailed description of interactions between solvent molecules at the atomic level. The use of explicit solvent models adds an extra level of complexity to the problem. Both solute-solvent and solvent-solvent interaction terms must be considered, which slow down the simulations.[87] In contrast, implicit models dispense with this detail by considering the solvent to be a dielectric continuum, and are

thus the more computationally efficient. The use of a continuum approximation can be justified by realizing that it is not necessary to know every detail about concerning the solvent. It is only important to know how to model the solvent effects on the properties of interest. Specially, it is unnecessary to quantify interactions between individual water molecules in the bulk solvent. At the simplest level, where the properties of the solvent are determined by a dielectric constant, only knowledge of the noncovalent interactions between the solute and solvent molecules is required to compute solvation properties.[88-90]

Although force fields have been well established, we have noticed that problems have occurred from the lack of a correct balance between the solute-solute interactions and solute-solvent interactions.[91] Recently, Kirkwood-Buff theory has been used to quantify solute-solute and solute-solvent interactions in solution mixtures over the entire range of composition.[92-93]

1.3 Kirkwood-Buff Theory

1.3.1 Introduction

Our interest in KB theory is led by the desire to use computer simulation to study cosolvent effects at the atomic level and to apply KB theory to analyze the results. Other theories cannot provide satisfactory results concerning solution behavior over the whole concentration range, even with well developed models. Solution behavior has received much attention during this century because of its wide application in science, industry and environment. The focus of our research is to express the preferential interactions and associated activity derivatives by KB integrals which can be obtained from experiment or simulation. This is the most promising recent approach to help us understand cosolvent effects in solution.

Kirkwood-Buff theory is one of the most important theories of solutions and was published in 1951 by Kirkwood and Buff.[94] This theory was developed on the basis of statistical theory, originally formulated to obtain macroscopic thermodynamic properties from molecular distribution functions, providing a direct relationship to thermodynamic properties such as isothermal compressibility, partial molar volumes and derivatives of the chemical potentials.[95,96]

As mentioned above, the goal of KB theory is to compute the macroscopic thermodynamic properties based on the radial distribution function (see below). However, it was not that popular until a dramatic turning point – the inversion of KB theory occurred. The inversion of KB theory (Ben-Naim 1978) provides experimental information about the affinity between a pair of species in the solution mixture as extracted from measurable thermodynamic data.[97] As it is relatively easy to measure the required thermodynamic properties, the inversion procedure provides a new and powerful tool to investigate the characteristics of the local environments of each species in a multicomponent system.

A radial distribution function (rdf) provides the probability of finding a particle *j* at a distance *r* from another particle *i* at a distance r relative to the corresponding bulk solution. To calculate the *g(r)* for the particle 1 and 2 in a system of N particles, we can express it as,[98]

$$g_{12}(r) = \frac{\int ... \int e^{-\beta V_N} dr_3 dr_4 ... dr_N}{N^2 \int ... \int e^{-\beta V_N} dr_1 dr_2 ... dr_N} \qquad (1.10)$$

where $\beta = 1/kT$, and V_N is the potential energy of N particles. We obtain this equation by integration of the configurational distribution over the position of two atoms and then normalize. From the equation above, we may say that the rdf is a function of *r*, which also depends on P, T and composition.

In Figure 1.2, a plot of a typical radial distribution function is provided. At short distances, g_{ij} is zero because of strong repulsive forces between the two atoms/molecules. The first large peak occurs at about 0.25 nm**.** This means that it is four times more likely that two molecules *i* and *j* would be found at this separation than expected from a random distribution. The presence of the first solvation shell tends to exclude particles that are closer than the radius of the second solvation shell. As the distance between species i and j gets larger, g_{ij} goes to unity beyond R, meaning the distribution becomes similar to the bulk distribution**.**

Figure 1. 2 Radial distribution function (rdf). The rdf displays the local solution structures for species i and j as a function of distance r_{ij}.

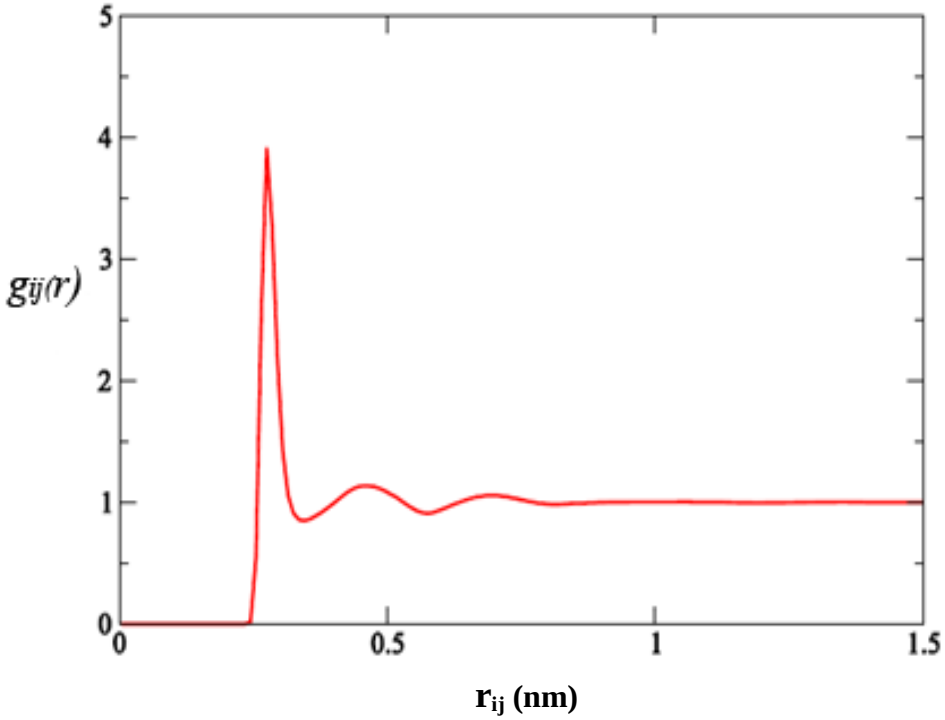

In the KB theory, thermodynamic properties can be expressed in the terms of KB integrals. We define the KB integral as,[99-101]

$$G_{ij} = 4\pi\int_0^{\infty}\left[g_{ij}^{\mu VT}(r)-1\right]r^2dr \approx 4\pi\int_0^{R}\left[g_{ij}^{NpT}(r)-1\right]r^2dr \qquad (1.11)$$

where $g_{ij}(r)$ is the radial distribution function. The volume of the spherical shell is $4\pi r^2 dr$ and r is the center of mass to center of mass distance. R is a cutoff distance at which the rdfs are essentially unity. From the equation above, we can see that KB integrals are sensitive to small deviations from the bulk distribution at large separations due to the r^2 weighting factor. The rdf provides the probability of finding a particle j in the distance r from another particle i in the grand canonical (μ, V, T) ensemble where the volume (V), temperature (T), and chemical potential (μ) are constant for the two species i and j. Besides simulation, g_{ij} can be measured

Figure 1. 3 An example of a KB integral G_{ij} as a function of integration distance R_{ij} (nm) between species i and j.

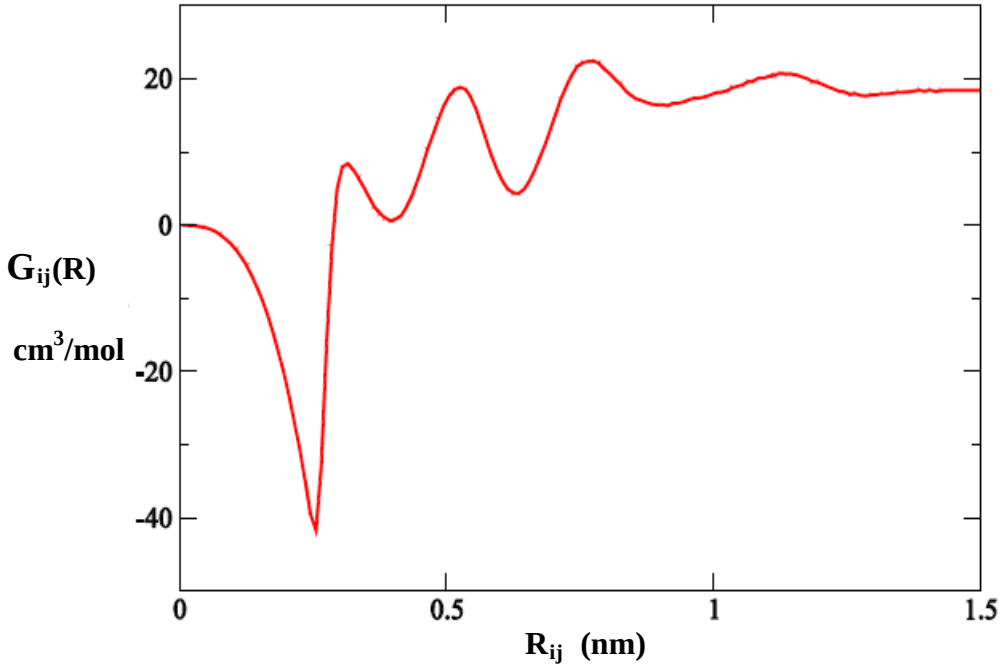

experimentally by X-ray or neutron scattering.[102,103] Unfortunately, g_{ij} is defined in open systems by KB theory, but our simulation is performed in closed systems. We consider that the distribution in μVT (open) ensemble is closely related to the distribution in the NpT (closed) ensemble if both of the systems are at the same composition, pressure and temperature. The assumed similarity between the closed and open system rdfs is based on the fact that the rdfs are primarily determined by the interactions between particles at short range. As pointed out by Ben-Naim, only the long-range behavior of the μVT and NpT rdfs are fundamentally different.[97] Fortunately, this is a negligible quantity except when the integration over the rdf extends to infinity. Here, the approximation is made for simulation performed in closed systems.[101,104]

The KB integrals are symmetric with respect to the interchange of indices i and j, $G_{ji}=G_{ij}$. The excess coordination number,

$$N_{ij} = \rho_j G_{ij}, \quad \rho_j = N_j / V \tag{1.12}$$

where ρ_j is the number density of species j in the system, is not symmetric, that is $N_{ij} \neq N_{ji}$, because $N_{ij}= \rho_j G_{ij}$ and $N_{ji}= \rho_i G_{ji}$. The excess coordination number represents the excess ($N_{ij} > 0$) or deficit ($N_{ij} < 0$) over a random distribution of j molecules in the vicinity of the central i molecule.[105]

For a two-component system consisting of water (w) and a cosolvent (c), the partial molar volumes of the two components, $\overline{V_c}$ and $\overline{V_w}$, the isothermal compressibility of the solution, κ_T, and the derivatives of the cosolvents activity a_{cc} can be expressed in terms of the integrals G_{ww}, G_{cc} and G_{cw} and the number densities ρ_w and ρ_c, of water and cosolvent,[104]

$$\overline{V_w} = \frac{1+\rho_c(G_{cc}-G_{cw})}{\eta} \tag{1.13}$$

$$\overline{V_c} = \frac{1+\rho_w(G_{ww}-G_{cw})}{\eta} \tag{1.14}$$

$$a_{cc} = \left(\frac{\partial \ln a_c}{\partial \ln \rho_c}\right)_{p,T} = 1+\left(\frac{\partial \ln y_c}{\partial \ln \rho_c}\right)_{p,T} = \frac{1}{1+\rho_c(G_{cc}-G_{cw})} \tag{1.15}$$

Figure 1. 4 An example of excess coordination number N_{ij} for different concentrations of solutes. The sign of N_{ij} indicates the nature of the intermolecular interactions between species i and j: positive N_{ij} indicates attractive interactions between i and j, while negative N_{ij} represent repulsive interactions.

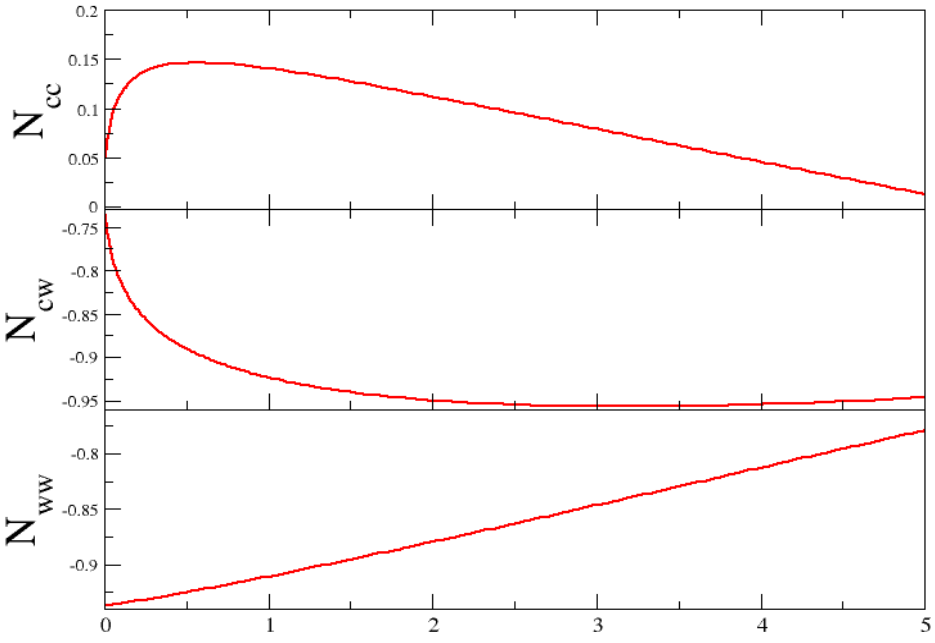

where $\eta = \rho_w + \rho_c + \rho_w\rho_c(G_{ww} + G_{cc} - 2G_{cw})$, $a_c = y_c\rho_{c,}$ and ρ_c is the number density or molar concentration. KB theory cannot be applied directly to the study of salt solutions because of a slight complication. As a consequence of the electroneutrality conditions, it is not possible to consider the salt solution as a ternary system of cations, anions, and water. Let us take sodium chloride as example. We cannot obtain derivatives of the sodium or chloride ion chemical potentials or activities. However, it is possible to treat the salt solution as a binary system of indistinguishable ions and water.[106-108] We have chosen to treat the anions and cations of salts as indistinguishable particles to apply the KB equations for a binary solution (water and cosolvent). Hence, we distinguish between the usual molar salt concentration m_s and the concentration of indistinguishable ions $\rho_c = n_{\pm}C_c$, for which $n_{\pm} = n_+ + n_-$ is the number of ions produced on dissociation of the salt.

Figure 1. 5 A simple chart displaying how KB theory works with our research. By comparing KB integrals, excess coordination numbers, or other thermodynamic properties between experiment and simulation, we can determine the disparity between reality and our force field.

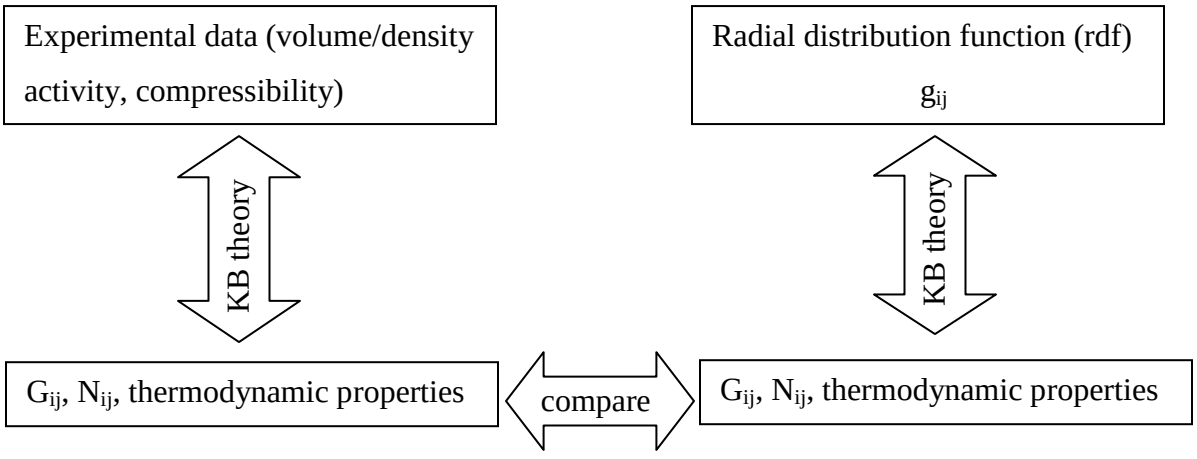

1.3.2 Kirkwood – Buff Derived Force Field

KB integrals have proved to be a good tool to probe the interactions between particles.[109-115] Many existing force fields display poor performance in reproducing these integrals and therefore lead to inaccurate simulations. Consequently, there is a constant need for improved force fields. We have been developing a series of force fields which were specifically designed to reproduce the experimental KB integrals obtained from the experimental data. These KB derived force fields (KBFF) have been shown to reasonably reproduce not only the KB integrals, but also other thermodynamic and physical properties of aqueous solution mixtures.[116-122]

The Kirkwood-Buff derived Force Field (KBFF) is still a non-polarizable force field. But the KB integrals are very sensitive to the force field parameters, particularly to the charge distribution. Therefore, to develop this force field, we focus on developing accurate charge distributions for atoms. The Kirkwood-Buff derived force field involves a Lennard-Jones (LJ) 6-12 plus Coulomb potential. The water model applied with this force field is SPC/E.[123] The molecular geometry is normally taken from the available crystal structures, with bonded parameters taken from the GROMOS96 force field.[124] The charges on each atom are then adjusted to reproduce the density and KB integrals for solution mixtures. A list of Kirkwood-Buff derived force fields is shown as follows,

Urea	Weerasinghe and Smith, JCP, v118, 3891-3898, 2003
Acetone	Weerasinghe and Smith, JCP, v118, 10663-10670, 2003
NaCl	Weerasinghe and Smith, JCP, v119, 11342-11349, 2003
Guanidinium chloride	Weerasinghe and Smith, JCP, v121, 2180-2186, 2004
Methanol	Weerasinghe and Smith, JPCB, v109, 15080-15086, 2005

NMA	Kang and Smith, JCC, v27, 1477-1485, 2006
Thiols, sulfides, disulfides	Bentenitis, Cox, and Smith, JPCB, v113, 12306-12315, 2009

1.3.2 Advantages & Disadvantages

KB theory has been used extensively in the chemistry and chemical engineering fields to provide information on intermolecular distributions and preferential solvation in solution.[105] It is important to realize that the specific advantages and disadvantages of KB theory include:[105]

1. It is an exact theory which does not involve any approximations.
2. KB theory can be applied to relate several thermodynamic properties in terms of KB integrals. Therefore, it provides more data for testing of a force field.
3. There is no limitation concerning the sizes of molecules used. Molecules can range from simple salt like sodium chloride, to organic molecules like methanol, even to biomolecules like urea.
4. It does not assume pairwise additivity of interactions. Many solution theories involve an approximation of pairwise additivity to decrease the computational demand. This approximation does not calculate the interaction between three or more atoms, only the sum of pairwise interaction. This kind of approximation can absolutely lead to differences between experimental and calculated results. KB theory avoids this drawback.
5. It can be applied to any stable solution mixture involving any number of components. But, it is widely realized that the relationships between the thermodynamic properties and KB integrals get more complicated as the number of components in a system increases, since more components are involved in the matrix operations.

1.4 The Aims of this Thesis

The aims of the group include the study of the effects of solvent and cosolvents on the structure and dynamics of biomolecules in solution by means of molecular dynamics simulations which are used to provide atomic level detail concerning the properties of these molecules using experimental data. The goal is to understand this behavior using theoretical calculations, analyzing, representation, and manipulation of 3D molecular structures. These approaches allow us to gain new ideas and reliable working hypotheses for molecular interactions in complexes of biological relevance. Here, the applicability of these techniques is shown in the study of :

1. Interactions of tetrahedral ions with water molecules
2. Interactions of trigonal planar ions with water molecules

Kirkwood-Buff theory is used to quantify and balance ion-ion and ion-water interactions, and therefore provide the possibility to develop more accurate force fields for the simulation of solution mixtures.

Reference

1. Narumi, T.; Susukita, R.; Ebisuzaki, T.; McNiven, G. (1999). Molecular dynamics machine: special-purpose computer for molecular dynamics simulations. Molecular Simulation, 21(5&6), 401-415.
2. Frenkel, D.; Smit, B. (). Molecular simulation: from algorithms to application, 2nd edition.(pp.63-110). Academic Press.
3. Halie, J. M. (1992). Molecular dynamics simulation: elementary methods, 1st edition (pp. 24-30). John Wiley & Sons.
4. Giessibl, Franz J. (2003). Advances in atomic force microscopy. Reviews of Modern Physics , 75(3), 949-983
5. Allen M.P.; Tildesley, D. J. (1989). Computer Simulation of Liquids (pp. 283-289). Oxford University Press: Oxford.
6. Rapaport, D.C. (1995). The art of molecular dynamics simulation (pp. 1-10). Cambridge University Press.
7. Gee, M. B.; Smith, P. E.; (2009). Kirkwood-Buff theory of molecular and protein association, aggregation, and cellular crowding. J. Chem. Phys., 131(16), 165101-165111.
8. Bentenitis, N.; Cox, N. R.; Smith, P. E. (2009). A Kirkwood-Buff derived force field for thiols, sulfides, and disulfides. J. Phys. Chem. B, 113(36), 12306-12315.
9. Gibbs, G. W. (1981). Elementary principles in statistical mechanics (pp. 3-17). Woodbridge, Connecticut: Ox Bow Press.
10. Hoover, W. G. (1991). Computational statistical mechanics,1st edition. Elsevier Science Publishers Ltd.

11. Nicholson, D.; Parsonage, N. G.(1982). Computer simulation and the statistical mechanics of adsorption. Academic Press.
12. Chandler, D. (1987). Introduction to Modern Statistical Mechanics. Oxford University Press.
13. McQuarrie, D. (2000). Statistical Mechanics (2nd rev. Ed.). University Science Books.
14. Balbuena, Perla; Seminario, Jorge M. (1999). Molecular Dynamics, Volume 7: From Classical to Quantum Methods. Elsevier Science.
15. Atkins, P. W.; DePaula, J. (2003). Physical Chemistry, 7th edition. W.H. Freeman and Company: New York.
16. Alder, B. J.; Wainwright, T. E. (1959). Studies in Molecular Dynamics .1. General Method. Journal of Chemical Physics, 31 (2), 459-466.
17. Alder, B. J.; Wainwright, T. E. (1957). Phase Transition for A Hard Sphere System. Journal of Chemical Physics**,** 27 (5), 1208-1209.
18. Stillinger, F. H. and Rahman. (1974). Propagation of sound in water: A molecular-dynamics study. Phys. Rev.A, 10(1), 368-378.
19. McCammon, J. A., Gelin, B. R., and Karplus, M. (1977). Dynamics of folded proteins. Nature, 267, 585-591.
20. Alder, B. J.; Wainwright, T. E.(1959). Studies in molecular dynamics. I. general method. Journal of Chemical Physics, 31(2), 459-466.
21. Bopp, P. A.; Buhn, J. B.; Hampe, M. J. (2008). Scope and limits of molecular simulations, 195(1), 323-340.
22. Car, R.; Parrinello, M. (1985). Unified approach for molecular dynamics and density-functional theory. Phys. Rev. Lett., 55(22), 2471-2474).

23. Evans, D. J.; Murad, S. (1977). Singularity free algorithm for molecular dynamics simulation of rigid polyatomics. Molecular Physics, 34(2), 327-331.

24. Nose, S. (1984). A molecular dynamics method for simulations in the canonical ensemble. Molecular Physics, 52(2), 255-268.

25. Kosloff, R. (1988). Time-dependent quantum-mechanical methods for molecular dynamics. J. Phys. Chem., 92(8), 2087-2100.

26. Hardy, J.; Pazzis, O. de. (1976). Molecular dynamics of a classical lattice gas: Transport properties and time correlation functions. Phys. Rev. A, 13(5), 1949-1961.

27. Streett, W. B.; Tildesley, D. J.; Saville, G.(1978). Multiple time-step methods in molecular dynamics. Molecular Physics, 35(3), 639-648.

28. Metropolis, N.; Rosenbluth, A. W.; Rosenbluth, M. N.; Teller, A. H.; Teller, E. (1953). Equation of state calculations by fast computing machines. Journal of Chemical Physics, 21(6), 1087-1092.

29. Mosegaard, K.; Tarantola, A. (1995). Monte-Carlo Sampling of Solutions to Inverse Problems. Journal of Geophysical Research-Solid Earth, 100 (B7), 12431-12447.

30. Creutz, M. (1983). Microcanonical Monte carlo simulation. Phys. Rev. Lett., 50(19), 1411-1414.

31. Lee, J. (1993). New monte carlo algorithm: entropic sampling. Phys. Rev. Lett.; 71(2), 211-214.

32. Manousiouthakis, V. I.; Deem, M. W. (1999). Strict detailed balance is unnecessary in Monte Carlo simulation. J. Chem. Phys., 110(6), 2753-2758.

33. Hansmann, U. H. E.; Okamoto, Y.; Eisenmenger, F. (1998). Molecular dynamics , Langevin and hydrid Monte Carlo simulation in a multicanonical ensemble. Chemical Physics Letters, 259(3-4), 321-330.

34. Cichocki, B.; Ekiel-Jezewska, M. L.; Wajnryb, E. (1999). Lubrication corrections for three-paraticle contribution to short-time self-diffusion coefficients in colloidal dispersions. J. Chem. Phys. 111(7), 479605-479612.

35. Duncan, J. L.; Allan, A.; McKean, D. C. (1970). ^{13}C frequency shifts and the general harmonic force fields of methyl chloride, bromide and iodinde. Molecular Physics, 18(3), 289-303.

36. Duncan, J. L.; McKean, D. C.; Mallinson, P. D. (1973). Infrared crystal spectra of C_2H_4, C_2D_4, and as-$C_2H_2D_2$ and the general harmonic force field of ethylene. Journal of Molecular Spectroscopy. 45(2), 221-246.

37. Duncan, J. L.; Hamilton, E. (1980). An improved general harmonic force field for ethylene. Journal of Molecular Structure: Theochem, 76(1), 65-80.

38. Weiner, S.J.; Kollman, P.A.; Nguyen, D.T.; Case, D.A. J.(1986). An all atom force field for simulations of proteins and nucleic acids. Comput. Chem., 7(2), 230-252.

39. Brooks, B.R.; Bruccoleri, R.E.; Olafson, B.D.; States, D.J.; Swaminathan, S.; Karplus, M. (1983). CHARMM: A program for macromolecular energy, minimization, and dynamics calculations. J. Comput. Chem., 14, 187-218.

40. Jorgensen, W.L.; Tirado-Rives, J. (1988). The OPLS potential functions for proteins.Energy minimizations for crystals of cyclic peptides and crambin. J. Am. Chem.Soc., 110(6), 1657-1666.

41. Van Gunsteren, W.F.; Berendsen, H.J.C. Gromos Molecular Simulation Library, 1987

42. Yannas, I.V.; Louise, R. R. (1983). Evaluation of collagen crosslinking techniques. Strengh and Stiffness of Polymers. Artificial Cells, Blood Substitutes, and Biotechnology, 11(4), 293-318.

43. Kardomateas, G. A.; Yannas, I. V.Phil. Mag.(1985). A model for the different crazing behavior of amorphous polymer glasses. Philosophical Magazine A, 52(1), 39-50.

44. Yu, H. B.; Hansson, T.; van Gunsteren, W. F. (2003). Development of a simple, self-consistent polarizable model for liquid water. J. Chem. Phys., 118(1), 221-234.

45. Hess, B.; Saint-Martin, H.; Berendsen, H. J. C.(2002). Flexible constraints: An adiabatic treatment of quantum degrees of freedom, with application to the flexible and polarizable mobile charge densities in harmonic oscillators model for water. J. Chem. Phys., 116(22), 9602-9611.

46. Saint-Martin, H.; Hernandez-Cobos, J.; Bernal-Uruchurtu, M. L.; Ortega-Blake, I.; Berendsen, H. J. C. (2000). Mobile charge densities in harmonic oscillators (MCDHO) molecular model for numerical simulations: The water-water interaction. J. Chem. Phys. 113(24), 10899-10913.

47. Car, R.; Parrinello, M. (1985). Unified approach for molecular dynamics and density-functional theory. Phys Rev Lett, 55(22), 2471-2474.

48. Maple, J. R.; Dinur, U.; Hagler, A. T. (1988). Derivation of force fields for molecular mechanics and dynamics from ab initio energy surfaces. Pro. Natl. Acad. Sci., 85(15), 5350-5354.

49. Vorobyov, I. V.; Anisimov, V. M.; Mackerell A.D. Jr. (2005). Polarizable empirical force field for alkanes based on the classical drude oscillator model. J. Phys. Chem. B, 109(40), 18988-18999.

50. Ponder J.W. and Case D. A. (2003). Force fields for protein simulations. Adv. Prot. Chem. 66: 27-85

51. Lopes, J. N. C. (2004). Modeling ionic liquids using a systematic all-atom force field. J. Phys. Chem. B., 108(6), 2038-2047.

52. Jorgensen, W.L.; Maxwell, D.S., Tirado-Rives, J. (1996). Development and testing of the OPLS all-atom force field on conformational energetic and properties of organic liquids. J. Am. Chem. Soc., 118(45), 11225-11236.

53. Kaminski, G.; Friesner, R.A.; Tirado-Rives, J.; Jorgensen, W.L. (2001). Evaluation and reparametrization of the OPLS-AA force field for proteins via comparison with accurate quantum chemical calculations on peptides. J. Phys. Chem.B, 105(28), 6474-6487.

54. Schuler, L.D.; Daura, X.; van Gunsteren, W.F. (2001). An improved GROMOS96 Force field for aliphatic hydrocarbons in the condensed phase. J. Comput. Chem., 22(11), 1205-1219.

55. Neria, E.; Fischer, S.; Karplus, M.(1996). Simulation of activation free energies in molecular systems. J. Chem. Phys., 105(5), 1902-1922.

56. Peter R. Bergethon. (1998). The physical basis of biochemistry: the foundations of molecular biophysics.

57. Lin, H.; Truhlar, D. G. (2007). QM/MM: what have we learned, where are we, and where do we go from here? Theoretical Chemistry Accounts: Theory, Computation, and Modeling, 117(2), 185-199.

58. Mayo, S. L.; Olafson, B. D. Goddard, W. A. (1990). DREIDING: a generic force field for molecular simulations. J. Phys. Chem., 94(26), 8897-8909.

59. Levy, R. M.; Srinivasan, A. R.; Olson, W. K. (1984). Quasi-harmonic method for studying very low frequency models in proteins. Biopolymers, 23, 1099-1112.

60. Tuzun, R. E.; Noid, D. W.; Sumpter, B. G.(1998). Efficient treatment of out-of-plane bend and improper torsion interactions in MM2, MM3, and MM4 molecular mechanics calculations. J. Comp. Chem., 18(14), 1804-1811.

61. Nevins, N.; Allinger, N. L. (1998). Molecular mechanics (MM4) vibrational frequency calculations for alkenes and conjugated hydrocarbons. J. Comp. Chem., 17(5-6), 730-746.

62. Halgren, T. A. (1992). The representation of van der Waals (vdW) interactions in molecular mechanics force fields: potential form, combination rules, and vdW parameters. J. Am. Chem. Soc, 114(20), 7827-7843.

63. Tsuzuki, S.; Luthi, H. P. (2001). Interaction energies of van der Waals and hydrogen bonded systems calculated using density functional theory: Assessing the PW91 model. J. Chem. Phys., 114(9), 3939-3958.

64. Halgren, T. A. (1998). Merck molecular force field. II. MMFF94 van der Waals and electrostatic parameters for intermolecular interactions. J. Comp. Chem., 17(5-6), 520-552.

65. Oostenbrink, C.; Villa, A. E., van Gunsteren, W. F. (2004). A biomolecular force field based on the free enthalpy of hydration and salvation: the GROMOS force-field parameter sets 53A5 and 53A6. J. Comp. Chem., 25(13), 1656-1676.

66. Sharp, K. A.; Honig, B. (1990). Electrostatic interactions in macromolecules: theory and applications. Annu. Rev. Biophys. Biophys. Chem., 19, 301-332.

67. Momany. F. R. (1978). Determination of partial atomic charges from ab initio molecular electrostatic potentials. Application to formamide, methanol, and formic acid. J. Phys. Chem., 82(5), 592-601.

68. Tannor, D. J.; Marten B.; Murphy R.; Friesner, R. A.; Sitkoff, D.; Nicholls, A.; Honig, B. (1994). Accurate first principles calculation of molecular charge distributions and salvation energies from Ab initio quantum mechanics and continuum dielectric theory. J. Am. Chem. Soc., 116(26), 11875-11882.

69. Momany, F. A. (1978). Determination of partial atomic charges from ab initio molecular electrostatic potentials. Application to formamide, methanol, and formic acid. J. Phys. Chem., 82(5), 592-601.

70. Foresman, J. B Keith, T. A.; Wiberg, K. B. (1996). Solvent effects.5. Influence of cavity shape, truncation of electrostatics, and electron correlation on ab initio reaction field calculations. J. Phys. Chem., 100(40), 16098-16104.

71. Field, M. J.; Bash, P. A.; Karplus, M. (1989). A combined quantum mechanical and molecular mechanical potential for molecular dynamics simulations. J. Comp. Chem., 11(6), 700-733.

72. De Leeuw, S. W.; Perram J. W.; Smith, E. R.(1979). Simulation of electrostatic systems in periodic boundary conditions. I. Lattice sums and dielectric constants. Proc. R. Soc. Lond. A, 373, 27-56.

73. Makov, G. Payne. M. C. (1994). Periodic boundary conditions in ab initio calculations. Phys. Rev. B, 51(7), 4014-4022.

74. Grubmuller, H.; Heller, H.; Windermuth, A.; Schulten, K. (1991). Generalized verlet algotithm for efficient molecular dynamics simulations with long-range interactions. Molecular Simulation, 6(1-3), 121-142.

75. Madura, J. D.; Pettitt, B. M. (1988). Effects of truncation long-range interactions in aqueous ionic solution simulations. Chem. Phys. Lett., 150(1-2), 105-108.

76. Prevost, M.; Belle, D. V.; Lippens, G.; Wodak, S. (1990). Computer simulations of liquid water: treatment of long-range interactions. Molecular Physics, 71(3), 587-603.

77. Essmann, U.; Perera, L.; Berkowitz, M. L.(1995). A smooth particle mesh Ewald method. J. Chem. Phys., 103(19), 8577-8594.

78. Belhadj, M.; Alper, H. E.; Levy, R. M. (1991). Molecular dynamics simulations of water with Ewald summation for the long range electrostatic interactions. Chem. Phys. Lett., 179(1-2). 13-20.

79. Martyna, G. J.; Tuckerman, M. E.(1999). A reciprocal space based method for treating long range interactions in ab initio and force-field-based calculations in clusters. J. Chem. Phys., 110(6), 2810-2822.

80. Halgren, T. A.; Damm, W. (2001). Polarizable force field. Current Opinion in Structural Biology, 11(2), 236-242.

81. Stern, H. A.; Kaminski, G. A.; Banks, J. L.; Zhou, R.; Berne, B. J.(1999). Fluctuating charge, polarizable diple, and combined models: parameterization from ab initio quantum chemistry. J. Phys. Chem. B, 103, 4730-4737.

82. Banks, J. L.; Kaminski, G. A.; Zhou, R.; Mainz, D. T.; Berne, B. J.; Friesner, R. A. (1999). Parameterizing a polarizable force field from ab initio data. I. The fluctuating point charge model. J. Chem. Phys., 110, 741-754.

83. Applequist, J.; Carl, J. R.; Fung, K. K. (1972). An atom-dipole interaction model for molecular polarizability. Application to polyatomic molecules and determination of atom polarizabilities. J. Am. Chem. Soc., 94, 2952-2960.

84. Soetens, J. C.; Millot, C.; Chipot. C.; Jansen, G.; Angyan, J. G.; Maigret, B. (1997). Effect of polarizability on the potential of mean force of mean force of two cations. The guanidinium-guandinium ion pair in water. J. Chem. Phys. B, 101, 10910-10917.

85. Martin, M. G.; Chen, B.; Siepmann, J. I. (1998). A novel Monte Carlo algorithm for polarizable force fields: application to a fluctuating charge model for water. J. Chem. Phys., 108, 3383-3385.

86. van Belle, D.; Froeyen, M.; Lippens, G.; Wodak, S. J.(1992). Molecular dynamics simulation of polarizable water by extended Lagrangian method. Mol. Phys., 77, 239-255.

87. Levy, R. M.; Gallicchio, E. (1998). Computer simulations with explicit solvent: recent progress in the thermodynamic decomposition of free energies and in modeling electrostatic effects. Annu. Rev. Phys. Chem., 49, 531-567.

88. Feig, M.; Brooks, C. L. (2004). Recent advances in the development and application of implicit solvent models in biomolecules simulations. Current Opinion in Structural Biology, 12(2), 217-224

89. Gallicchio, E.; Levy, R. M. (2003). AGBNP: an analytic implicit solvent model suitable for molecular dynamics simulations and high-resolution modeling. J. Comp. Chem., 25(4), 479-500.

90. Baker, N. (2005). Improving implicit solvent simulations: a Poisson-centric view. Current Opinion in Structural Biology, 15(2), 137-143.

91. Smith, P. E. (2006). Chemical potential derivatives and preferential interaction parameters in biological systems from Kirkwood-Buff theory. Biophysical Journal, 91(3), 849-856.

92. Smith, P. E. (2006). Equilibrium dialysis data and the relationships between preferential interaction parameters for biological systems in terms of Kirkwood-Buff integrals. J. Phys. Chem. B., 110(6), 2862-2868

93. Chitra, R.; Smith, P. E. (2001). Preferential interactions of cosolvents with hydrophobic solutes. J. Phys. Chem. B., 105(46), 11513-11522.

94. Kirkwood, J. G.; Buff, F. P. (1951). The statistical mechanical theory of solutions. J. Chem. Phys., 19, 774-778.

95. Kirkwood, J. G.; Poirier, J. C. (1954). The statistical mechanical basis of the Debye-Huekel theory of strong electrolytes. J. Phys. Chem., 58(8), 591-596.

96. Hall, D. G.(1971). Kirwood-Buff theory of solutions. An alternative derivation of part of it and some applications. Trans. Faraday Soc., 67, 2516-2524.

97. Ben-Naim, A. (1977). Inversion of the Kirkwood-Buff theory of solutions: Application to the water-ethanol system. J. Chem. Phys., 67(11), 4884-4891.

98. McDonald, I. R.; Singer, K. (1972). An equation of state for simple liquids. Molecular Physics, 23(1), 29-40.

99. Chitra, R.; Smith, P. E. (2001). Properties of 2, 2, 2-trifluoroethanol and water mixtures. J. Chem. Phys., 114(1), 426-436.

100. Chitra, R.; Smith, P. E. (2002). Molecular association in solution: a Kirkwood-Buff analysis of sodium chloride, ammonium sulfate, guanidinium chloride, urea, and 2, 2, 2-trifluoroethanol in water. J. Phys. Chem. B, 106(6), 1491-1500.

101. Weerasinghe, S.; Pettitt, B. M. (1994). Ideal chemical potential contribution in molecular dynamics simulations of the grand canonical ensemble. Molecular Physics, 82(5), 897-912.

102. Filipponi, A. (1994). The radial distribution function probed by X-ray absorption spectroscopy. Journal of Physics: Condensed Matter, 6(41), 8415-8429.

103. Sorenson, J. M.; Hura, G.; Glaeser, R. M.; Gordon, T. H.(2000). What can x-ray scattering tell us about the radial distribution function of water? J. Chem. Phys., 113(20), 9149-9162.

104. Ben-Naim, A. (1992). Statistical Thermodynamics for chemicals and Biochemists. Plenum Press: New York.

105. Pierce, V.; Kang, M.; Aburi, M.; Weerasinghe, S.; Smith, P. E. (2007). Recent applications of Kirkwood-buff theory to biological systems. Cell Biochem Biophys, 50, 1-22.

106. Kusalik, P. G.; Patey, G. N. (1987). The thermodynamic properties of electrolyte solutions: some formal results. J. Chem. Phys., 86(9), 5110-5117.

107. Friedman, H. L.; Ramanathan, P. S. (1970). Theory of mixed electrolyte solutions and application to a model for aqueous lithium chloride-cesium chloride. J. Phys. Chem., 74(21), 3756-3765

108. Behera, R. (1998). On the calculation of thermodynamic properties of electrolyte solutions from Kirkwood-Buff theory. J. Chem. Phys., 108(8), 3373-3375.

109. Guha, A.; Mukherjee, D. (1997). Kirkwood-Buff parameter for the solubility of gases in water at high pressure. Journal of the Indian Chemical Society, 74(3), 195-198.

110. Guha, A.; Ghosh, N. K. (1998). Kirkwood-Buff parameters for the binary mixtures and determination of partial structure factor in the long waveleng limit. Indian Journal of Chemistry A- Inorganic Bio-Inorganic Physical Theoretical & Analytical Chemistry, 37(2), 97-101.

111. Kang, M.; Smith, P. E. (2006). A Kirkwood-Buff derived force field for amides. J. Comp. Chem., 27(13), 1477-1485.

112. Smith, P.E. (2008). On the Kirkwood-Buff inversion procedure. J. Chem. Phys., 129(12), 124509-124514.

113. Weerasinghe, S.; Smith, P. E. (2005). A Kirkwood-Buff derived force field for methanol and aqueous methanol solutions. J. Phys. Chem. B, 109(31), 15080-15086.

114. Weerasinghe, S.; Smith, P. E. (2004). A Kirkwood-Buff derived force field for the simulation of aqueous guanidinium chloride solutions. J. Chem. Phys., 121(5), 2180-2186.

115. Weerasinghe, S.; Smith, P. E. (2003). Kirkwood-Buff derived force field for mixtures of acetone and water. J. Chem. Phys., 118(23), 10663-10670

116. Weerasinghe, S.; Smith, P. E. (2003). A Kirkwood-Buff derived force field for mixtures of urea and water. J. Phys. Chem. B, 107(16), 2891-3898.

117. Imai, T.; Kinoshita, M.; Hirata, F. (2000). Theoretical study for partial molar volume of amino acids in aqueous solution: implication of ideal fluctuation volume. J. Chem. Phys., 112(21), 9469-9479.

118. Lynch, G. C.; Perkyns, J. S.; Pettitt, B. M. (1999). Kirkwood-Buff thermodynamics derived from grand canonical molecular dynamics and DRISM calculation. J. Comp. Phys., 151, 135-145.

119. Marcus, Y.(2001). Preferential salvation in mixed solvents X. Completely miscible aqueous co-solvent binary mixtures at 298.15K. Monatshefte fur chemie, 132(11), 1387-1411.

120. Matteoli, E. (1995).A simple expression for radial distribution functions of pure fluids and mixtures. 103, 4672-4677.

121. Pandey, J. D.; Verma, R. (2001). Inversion of the Kirkwood-Buff theory of solutions: application to binary systems. Chem. Phys., 270(3), 429-438.

122. Rosgen, J.; Pettitt, B. M.; Bolen, D. W. (2007). An analysis of the molecular origin of osmolyte-dependent protein stability. Protein Science, 16(4), 733-743.

123. Berendsen, H. J. C.; Grigera, J. R.; Straatsma, T. P. (1987).The missing term in effective pair potentials. J. Phys. Chem., 91, 6269-6271.

124. W. F. van Gunsteren, S. R. Billeter, A. A. Eising, P. H. Hunenberger, P. Kruger, A. E. Mark, W. R. P. Scott, and I. G. Tironi. (1996). Biomolecular Simulation: The GROMOS96 Manual and User Guide. vdf hochschulverlang, ETH zurich, Switzerland.

CHAPTER 2 - A Kirkwood-Buff Force Field for Polyoxoanions in Water

2.1 Introduction

The presence of ions plays a central role in changing intensive properties of the solution, such as viscosity, surface tension, relative permittivity, and molecular properties like diffusion constants.[1, 2] In addition, ions which are used as cosolvents influence largely the stability, solubility, conformational preferences and ligand binding of proteins. The addition of solutes or cosolvent molecules to water has a marked effect on the structure of water molecules by ion-water interaction, or when ions are bound to proteins directly.[3] Typically, cosolvents are classified as "kosmotropes" and "chaotropes" in terms of their ability to "create" or "destroy" water bulk structures, and are also used to refer to protein structure stabilizers and denaturants, respectively.[4,5]

It has been clearly demonstrated that cosolvent effects result from a competition between water-ion interaction and water-water interaction.[3] If water-ion interactions are stronger than water-water interactions, cosolvent ions will be excluded from the vicinity of the solute because of their preferential hydration. This leads to a decrease in the solubility of biomolecules in water. This phenomenon is referred to as salting-out. On the other hand, if water-ion interactions are weaker than water-water interactions, cosolvent ions may interact specifically with biomolecules, increasing their solubility, which is referred to as salting-in.[6-8]

The phenomenon of salting-in and salting-out was first reported by Hofmeister in 1888, who originally established a qualitative order as to how different ions affect the solubility of proteins in water. This order is known as the Hofmeister series.[9] Generally, ion effects on the

solubility of proteins are related to the charge densities of the ions. Ions with high charge densities tend to decrease the solubility, while ions with low charge densities tend to increase the solubility.[10] The Hofmeister series plays a central role in science and technology and substantial attention has been paid to it. The rank order in terms of effectiveness of the ions in salting out is shown below,[11]

Figure 2. 1 The Hofmeister Series for Anions

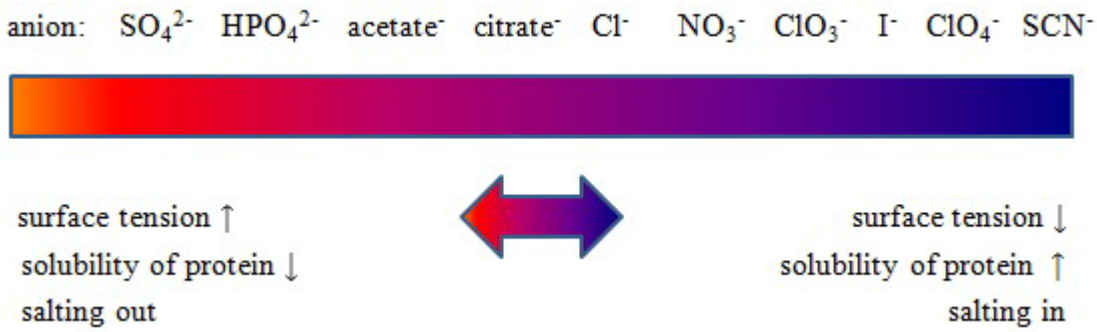

Anions appear to have a more pronounced effect than cations due to their more diffuse valence electronic configuration. In the above series for anions, ions on the left increase the surface tension of solvent and decrease the solubility of proteins (salting out). On the other hand, ions on the right decrease the surface tension and increase the solubility of proteins (salting in). In our research, we are trying to interpret the effects of cosolvents on the structure and solubility of biomolecules. Of all the properties of ions in solutions, perhaps the most fundamental are the solvation properties. A detailed understanding of electrolyte solutions requires knowledge of the ion solvation. We have undertaken a study of the properties of several common cosolvents in solution to investigate the changes in associations and interactions on addition of some common cosolvents.

Here, a KB analysis of salt solutions as a function of salt concentration is used to help the development of KB derived force fields for several anions. We present the results for a series of tetrahedral anions, like sulfate, perchlorate and phosphate ions, and trigonal planar anions, like nitrate and carbonate ions, which are quite important in biological systems and in the Hofmeister series. The tetrahedral and trigonal planar models are also important because their simple symmetric geometry makes them a good choice for understanding fundamental polyatomic ion-solvent interactions.

Ammonium sulfate and sodium sulfate are typical precipitants of proteins.[12] The hydrated sulfate ion is fundamental in a range of processes in biochemistry because of its rank in Hofmeister series. Sodium perchlorate is the precursor to many other perchlorate salts due to its relatively high solubility. Its effect on properties of solution is quite different from sulfate, as perchlorate bears a relatively low charge density, although it has the same geometry as sulfate.[13] The properties of phosphate ions are crucial in science and technology, like the manufacture of water softeners, in the rust-proofing process, and for scouring powders.[14] In biological systems, phosphates are most commonly found in the form of adenosine phosphate. The addition and removal of the phosphate from protein in all cells is a crucial strategy in the regulation of metabolic processes, such as in the production and function of ATP.[15] Phosphate and its protonated forms hydrogen phosphate, dihydrogen phosphate and phosphoric acid are of great relevance for physiological reactions as well as for industrial and agricultural application.[16] Phosphate rather than its protonated forms was chosen to be investigated here because of its similarity to the isoelectric ions sulfate and perchlorate.

The choice of force field is critical for describing accurately any system of interest by computer simulation. The accuracy of a force field is usually determined by comparing physical

properties between experiments and simulations. Force field parameters vary depending on the particular force fields. Our group has been developing a Kirkwood-Buff derived force field for molecular dynamics simulation to reproduce KB integrals obtained from the experimental data. Force field parameters for ammonium and sulfate have also been developed previously by Singh et al[17] and Cannon et al,[18] respectively. However, by KB analysis it will be demonstrated that those parameters do not correctly reproduce the correct solution activities (see later), which prompted our determination to develop new improved models.

2.2 Methods

2.2.1 Kirkwood-Buff theory

KB theory is commonly used to relate integrals over molecular distributions to macroscopic properties. It is important to realize that KB theory does not involve any approximations or limitations concerning the size or character of the molecules. The KB integrals are defined by,[19-21]

$$G_{ij} = 4\pi\int_0^\infty \left[g_{ij}^{\mu VT}(r) - 1 \right] r^2 dr \qquad (2.1)$$

where $g_{ij}^{\mu VT}(r)$ is the radial distribution function (rdf) between i and j in the grand canonical (μVT) ensemble. The above integrals provide a quantitative estimate of the affinity between species i and j in solution, above that expected for a random distribution. A positive value of the corresponding excess coordination number ($N_{ij} = \rho_j G_{ij}$) typically indicates an excess number of j molecules around a central i molecule, whereas a negative value indicates a depletion or exclusion of j molecules from the vicinity of i molecule.

The above integrals involve rdfs corresponding to an open (μVT) system. KB theory uses

these integrals to determine properties for a closed (NPT) system at the same density via suitable thermodynamic transformations. A variety of thermodynamic quantities can be defined in terms of the KB integrals G_{ww}, G_{cc}, and $G_{cw}=G_{wc}$. For a two-component system consisting of water (w) and a cosolvent (c), the partial molar volumes of the two components, $\overline{V_c}$ and $\overline{V_w}$, the isothermal compressibility of the solution, κ_T, and the derivatives of the cosolvents activity a_{cc} can be expressed in terms of the integrals G_{ww}, G_{cc} and G_{cw} and the number densities ρ_w and ρ_c, of water and cosolvents,[21]

$$\overline{V_w} = \frac{1+\rho_c(G_{cc}-G_{cw})}{\eta} \tag{2.2}$$

$$\overline{V_c} = \frac{1+\rho_w(G_{ww}-G_{cw})}{\eta} \tag{2.3}$$

$$a_{cc} = \left(\frac{\partial \ln a_c}{\partial \ln \rho_c}\right)_{p,T} = 1+\left(\frac{\partial \ln y_c}{\partial \ln \rho_c}\right)_{p,T} = \frac{1}{1+\rho_c(G_{cc}-G_{cw})} \tag{2.4}$$

where $\eta = \rho_w + \rho_c + \rho_w\rho_c(G_{ww}+G_{cc}-2G_{cw})$, $a_c = y\,\rho_c$, ρ_c is the number density or molar concentration, and a_c is the activity coefficient. KB theory cannot be applied directly to the study of salt solutions because of a slight complication. As a consequence of the electroneutrality conditions, it is not possible to consider the salt solution as a ternary system of cations, anions, and water. Let us take sodium chloride as example. We cannot obtain derivatives of the sodium or chloride ion chemical potentials or activities. However, it is possible to treat the salt solution as a binary system of indistinguishable ions and water.[22] We have chosen to treat the anions and cations of salts as indistinguishable particles to apply the KB equations for a binary solution (water and cosolvent). Hence, we distinguish between the usual molar salt concentration of

solute C_c and the concentration of indistinguishable ions $\rho_c = n_{\pm} C_c$, for which $n_{\pm} = n_+ + n_-$ is the number of ions produced on dissociation of the salt.[23,24]

Alternatively, KB integrals can be determined from experimental quantities (densities, partial molar volumes, compressibilities, and activity coefficient derivatives) using an inversion procedure,[20, 25]

$$G_{cw} = RT\kappa_T - \frac{\overline{V_w}\,\overline{V_c}}{DV_m} \tag{2.5}$$

$$G_{ww} = G_{cw} + \left(\frac{\overline{V_c}}{D} - V_m\right)\frac{1}{x_w} \tag{2.6}$$

$$G_{cc} = G_{cw} + \left(\frac{\overline{V_w}}{D} - V_m\right)\frac{1}{x_c} \tag{2.7}$$

where $D = 1 + x_c\left(\partial \ln f_c / \partial x_c\right)_{p,T} = 1 + x_w\left(\partial \ln f_w / \partial x_w\right)_{p,T}$, V_m is the molar volume of the solution, f_i is the activity on the mole fraction scale, x_i is the mole fraction of species i, and R is the gas constant. Experimental data like compressibilities, densities and activity coefficients are directly obtained from reference. These experimental data further produces experimental partial molar volumes and activity derivatives.

2.2.2 Molecular dynamics simulations

All solutions were simulated using derived Kirkwood-Buff force fields together with the SPC/E water model[26] as implemented in the GROMACS 4.0.5 package.[27-29] The simulations were performed in the isothermal isobaric ensemble at 300K and 1 atm. The weak coupling technique was used to modulate the temperature and pressure with relaxation times of 0.1 and 0.5 ps, respectively.[30] All anion bonds were constrained using SHAKE[31]and a relative tolerance of 10^{-4}, allowing a 2 fs time step for integration of the equation of motion, while water molecules were

constrained using the SETTLE[32] technique. The Particle Mesh Ewald technique was used to evaluate electrostatic interactions.[33] The twin range cutoffs is 0.8 (Coulomb) and 1.5 nm (van der Waals), with a nonbonded update frequency of 10 steps. Random initial configurations of molecules in a cubic box were used. Initial configurations of the different solutions were generated from a cubic box (L≈6 nm) of equilibrated water molecules by randomly inserting salt ions until the required concentration was attained. The steepest descent method was then used to perform minimization. This was followed by extensive equilibration, which was continued until all intermolecular potential energy contributions and rdfs displayed no drift with time. Total simulation times were typically 6 ns, and the final 5 ns were used for calculating ensemble averages. Configurations were saved every 0.1 ps for the calculation of various properties. Translational self-diffusion constants (D_i) were determined using the mean square fluctuation approach,[34] and relative permittivities from the dipole moment fluctuations.[35]

2.2.3 Parameter development

The KBFF model is a simple classical nonpolarizable force field designed for use with the SPC/E water model.[26] The approximation to the nonbonded potential energy in this study corresponded to the sum of Lennard-Jones (LJ) 6-12 plus Coulomb potential. In this scheme each pair of atoms i and j interact with an interaction energy given by

$$V_{ij} = \frac{q_i q_j}{4\pi\varepsilon_o r_{ij}} + 4\varepsilon_{ij}\left[\left(\frac{\sigma_{ij}}{r_{ij}}\right)^{12} - \left(\frac{\sigma_{ij}}{r_{ij}}\right)^{6}\right] \tag{2.8}$$

where all the symbols have their usual meaning and have been explained in the previous chapter.[36] The first term is the Coulombic interaction energy, and the second one is the corresponding van der Waals energy. The system potential energy is the sum of energies between all pairs of atoms i and j. Here, i and j are in different molecules. Figure 2.2 provides a

flow chart as to how we develop parameters for simulation. Firstly, we obtain the bonded parameters from experimental data or other available force field to determine geometry. The

Figure 2. 2 Flow chart for parameter development via simulation.

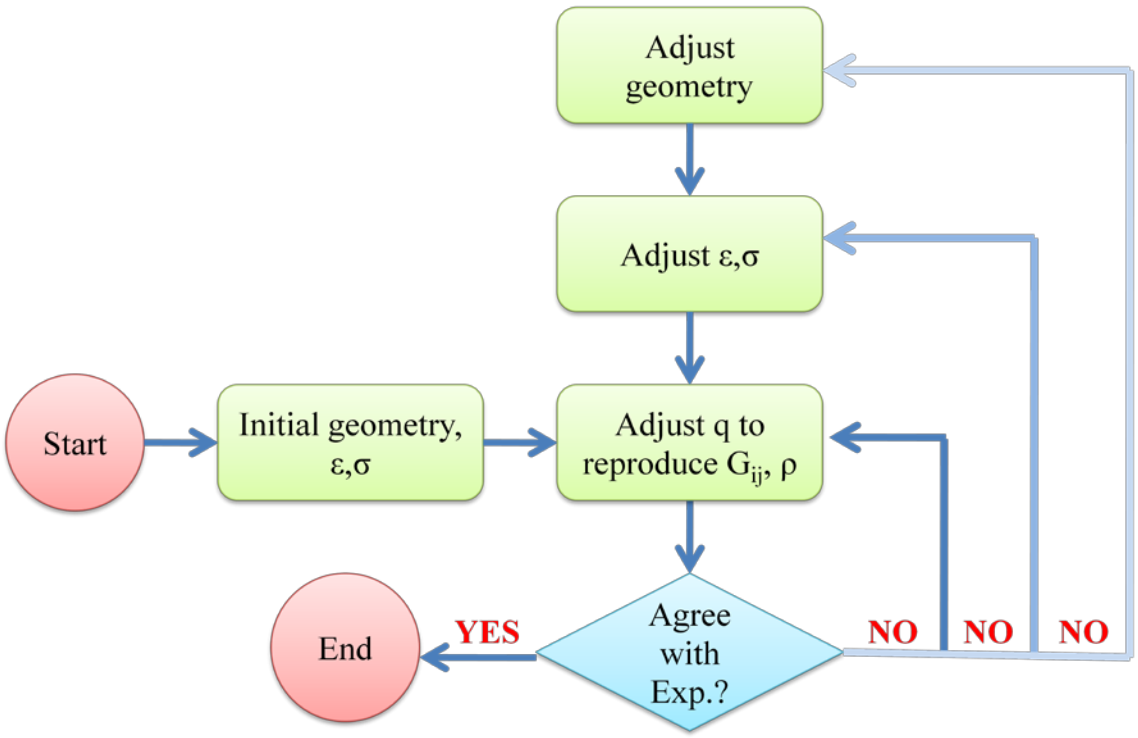

bonded parameters used in this study are presented in Table 2.1. Equilibrium bond lengths were set to the average values from crystal structures; equilibrium angles were taken from the GROMOS 96 43a1 force field.[37] Anions with tetrahedral and trigonal planar structures have angles of 109.5 ^{o} and 120^{o}, respectively. Then, we studied results for nonbonded parameters from existing force fields for the solution of interest if available. Nonbonded parameters for ammonium sulfate were taken from the existing force fields at the beginning; they are shown in Table 2.2. Charges on each atom were then adjusted to reproduce the KB integrals. However, this procedure alone could not provide reasonable values for the desired KB integrals.

Table 2. 1 Bonded force field parameters used in the simulations

Model	Bond		Reference
	Type	r_o(nm)	
NH_4^+	N-H	0.1000	GROMOS96
	H-H [a]	0.1633	
ClO_4^-	Cl-O	0.1426	38
	O-O [a]	0.2327	
SO_4^{2-}	S-O	0.1489	18
	O-O [a]	0.2433	
PO_4^{3-}	P-O	0.153	39
	O-O [a]	0.2499	
NO_3^-	N-O	0.1269	40
	O-O [a]	0.2197	
CO_3^{2-}	C-O	0.129	37
	O-O [a]	0.2234	

a. Artificially constrained to provide a rigid ion geometry

Table 2. 2 Nonbonded force field parameters for ammonium sulfate aqueous solution obtained from literature force fields.

Model	Atom	ε (kJ/mol)	σ (nm)	q (e)	References
NH_4^+	N	0.8368	0.3385	-0.896	17
	H	0	0	+0.474	
SO_4^{2-}	S	1.0460	0.3550	+2.4	18
	O	1.0460	0.3150	-1.1	
SPC/E	O	0.6506	0.3166	-0.8476	26
	H	0	0	+0.4238	

Table 2. 3 Comparison of the KBIs and properties of $(NH_4)_2SO_4$ solutions obtained with different literature force fields with experimental data.

m_s (mol/kg)		G_{cc} (cm^3/mol)	G_{ww} (cm^3/mol)	G_{cw} (cm^3/mol)	ρ (g/cm^3)	a_{cc}
2	EXP	60	-14	-34	1.119	0.67
	TRY01 [a]	2952	32	-399	1.127	0.05
	TRY02 [b]	1464	-4	-155	1.168	0.1
	TRY03 [c]	745	-5	-114	1.142	0.18
4	EXP	28	-9	-41	1.197	0.61
	TRY01 [a]	598	29	-187	1.226	0.12
	TRY02 [b]	36	-14	-32	1.292	0.59
	TRY03 [c]	46	-9	-42	1.237	0.54

a. NH_4^+ (Singh et al) + SO_4^{2-} (Cannon et al)

b. NH_4^+ (KBFF) + SO_4^{2-} (Cannon et al)

c. NH_4^+ (KBFF) + SO_4^{2-} (KBFF)

Figure 2. 3 Snapshot of 4m $(NH_4)_2SO_4$ aqueous solution without water molecules for different literature models. S (yellow), O (red), N (blue), H (white). a) TRY01, b) TRY02, c) TRY03.

a)

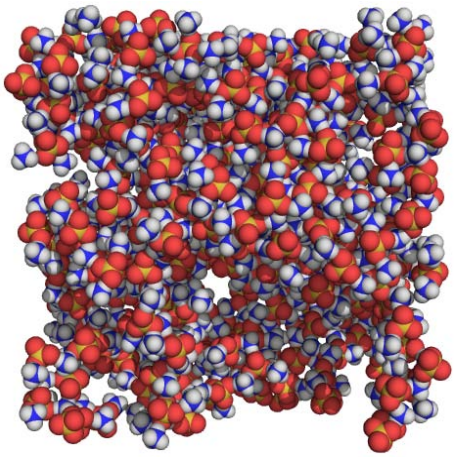

b)

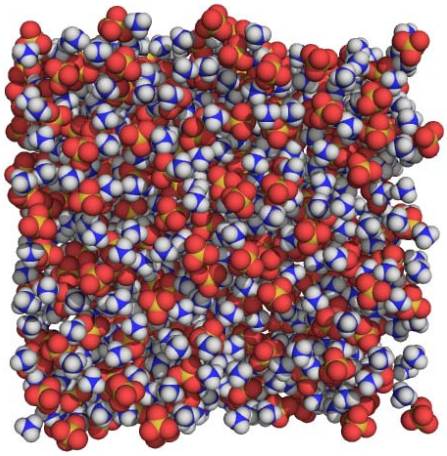

c)

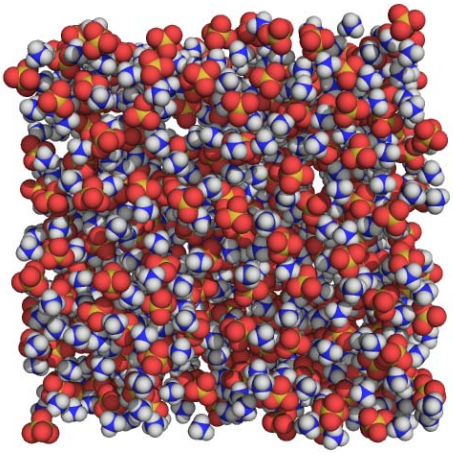

Consequently, we then changed the nonbonded parameters for the ammonium cation to the Kirkwood-Buff force field (KBFF) models which were developed previously by Smith group for

ammonium halide systems. [17,18] This provided an obvious improvement in the KB integrals but makes the density result worse at the same time. Subsequently, using our ammonium models, we replaced the Cannon et al oxygen by the KBFF oxygen which has more sp^3 property rather than sp^2. Changes to the ammonium and oxygen parameters provide satisfying simulation results for the KBIs (KB integrals) and other thermodynamic properties of 4M $(NH_4)_2SO_4$ aqueous solutions (see TRY03). A comparison of results by different parameters is displayed in Table 2.3. They show that only the KBFF could reproduce the KBIs and density at 4M. While the Singh et al ammonium model caused large aggregation, where the G_{cc} value was far more positive than expected (see Figure 2.3) and the Cannon et al sulfate model could not provide a reasonable simulated density.

We then directly applied the nonbonded parameters of sulfate developed in aqueous ammonium sulfate solution to sodium sulfate solution. For sodium perchlorate and sodium nitrate, the nonbonded vdws parameters (ε, σ) were obtained directly from previous KBFF models[39,41], and then adjust the charge distribution to fit the KB data. Finally, parameters for phosphate and carbonate have not been determined yet in this work for reasons that will become clear later.

2.3 Results and Discussion

Final nonbonded parameters for $(NH_4)_2SO_4$, Na_2SO_4, $NaNO_3$ and $NaClO_4$ are displayed in Table 2.4. A range of molecular simulations were performed and are summarized in Table 2.5**.** A KB analysis of the experimental data was performed using the available activity coefficients, density, and a simple approximation for the isothermal compressibility to provide target data for the simulations.

The simulated and experimental properties of $(NH_4)_2SO_4$, Na_2SO_4, $NaClO_4$, $NaNO_3$ at different concentrations are provided in Table 2.6. In order to further make sure the atoms are of the correct size, we have used the experimental crystal lattice dimensions to guide our parameter development for $(NH_4)_2SO_4$. The lattice simulation resulted in lattice constants of a=0.739, b= 1.0513, and c=0.6017 nm, compared to the experimental lattice parameters of a=0.7782, b=1.0636, and c=0.5993 nm, respectively.[45] Figure 2.4 displays the crystal lattice after 1 ns of simulation. The results were in reasonable agreement with experiment considering the simple Lennard-Jones 6-12 plus Coulomb potential used here.

Table 2. 4 Final KBFF nonbonded force field parameters used in the simulations

Model	Atom	ε (kJ/mol)	σ (nm)	q (e)	Reference
NH_4^+	N	0.562	0.337	+0.2	KBFF
	H	0.088	0.158	+0.2	
Na	Na	0.32	0.245	+1	42
ClO_4^-	Cl	0.47	0.44	+1.4	42
	O	0.56	0.31	-0.6	44
SO_4^{2-}	S	1.046	0.355	+2.4	18
	O	0.6047	0.35	-1.1	KBFF
NO_3^-	N	0.5	0.311	-0.4	43
	O	0.56	0.31	-0.2	44
SPC/E	O	0.6506	0.3166	-0.8476	26
	H	0	0	+0.4238	

Table 2. 5 Summary of the MD simulation performed here

	N_s	N_w	m_s(mol/kg)	V $(nm)^3$	E_{pot} (kJ/mol)	T_{sin} (ns)
$(NH_4)_2SO_4$	369	6804	1	213.788	-75.10	6
	690	6381	2	211.262	-99.37	6
	963	5951	3	207.960	-119.46	6
	1221	5645	4	208.707	-139.19	6
Na_2SO_4	381	7023	1	212.823	-82.18	6
	741	6854	2	212.275	-115.68	6
	1089	6718	3	213.844	-148.51	6
	1431	6608	4	217.908	-161.31	6
$NaClO_4$	250	6903	1	217.141	-57.88	6
	676	6248	3	213.759	-78.21	6
	1038	5769	5	213.089	-96.17	6
Na_3PO_4	260	7198	0.5	—	—	6
$NaNO_3$	254	7060	1	216.442	-58.86	6
	704	6518	3	210.620	-80.97	6
	1098	6100	5	209.171	-100.35	6
Na_2CO_3	384	7148	1	—	—	6
	759	7041	2	—	—	6
	1122	6941	3	—	—	6

Table 2. 6 Simulated and experimental properties of salt solutions

	m_s (mol/kg)		G_{cc} (cm^3/mol)	G_{ww} (cm^3/mol)	G_{cw} (cm^3/mol)	ρ (g/cm^3)	a_{cc}
$(NH_4)_2SO_4$	2	EXP	60	-14	-34	1.119	0.67
		SIM	745	-5	-114	1.142	0.18
	4	EXP	28	-9	-41	1.197	0.61
		SIM	46	-9	-42	1.237	0.54
Na_2SO_4	2	EXP	88	-17	-11	1.218	0.61
		SIM	626	-15	-43	1.24	0.21
	4	EXP	5	-17	-10	1.435	0.86
		SIM	88	-13	-32	1.423	0.43
$NaClO_4$	1	EXP	-7	-17	-23	1.070	0.97
		SIM	-7	-17	-23	1.068	0.97
	3	EXP	-51	-17	-19	1.195	1.20
		SIM	-85	-18	-13	1.196	1.60
	5	EXP	-58	-17	-15	1.300	1.50
		SIM	-74	-19	-10	1.305	2.10
$NaNO_3$	1	EXP	72	-17	-17	1.050	0.85
		SIM	70	-17	-12	1.057	0.86
	3	EXP	14	-17	-19	1.143	0.85
		SIM	14	-17	-17	1.161	0.85

5	EXP	2	-16	-20	1.221	0.84
	SIM	3	-16	-20	1.242	0.84

Unfortunately, KBFF models for $(NH_4)_2SO_4$ and Na_2SO_4 could not accurately reproduce the desirable results at low concentrations. The simulated G_{cc} was much higher than the experimental one, suggesting a large degree of ion aggregation. This is shown in Figure 2.5. According to dynamic light scattering, it has been shown that aqueous undersaturated solutions of ammonium sulfate indeed contain large ion clusters in water.[46] In the KB analysis of the simulation data, the distance at which the rdf is essentially unity was set to 1.5 nm. But actually, in $(NH_4)_2SO_4$ at 2M, the value of g_{cc} is not unity at 1.5 nm as shown in Figure 2.6. To further investigate this issue, we increased the box size from 6 nm to 12 nm and finally to 24 nm. In Figure 2.7, one can see that the oscillations of g_{cc} are getting smaller with increasing distance, suggesting that it would finally approach unity, but only if the box size was very large. Hence, the simulated data suggest large aggregation over long distances could be a feature of these systems, and render the value of G_{cc} meaningless in small systems.

Figure 2. 4 Snapshot of $(NH_4)_2SO_4$ crystals after simulating with our KBFF model.

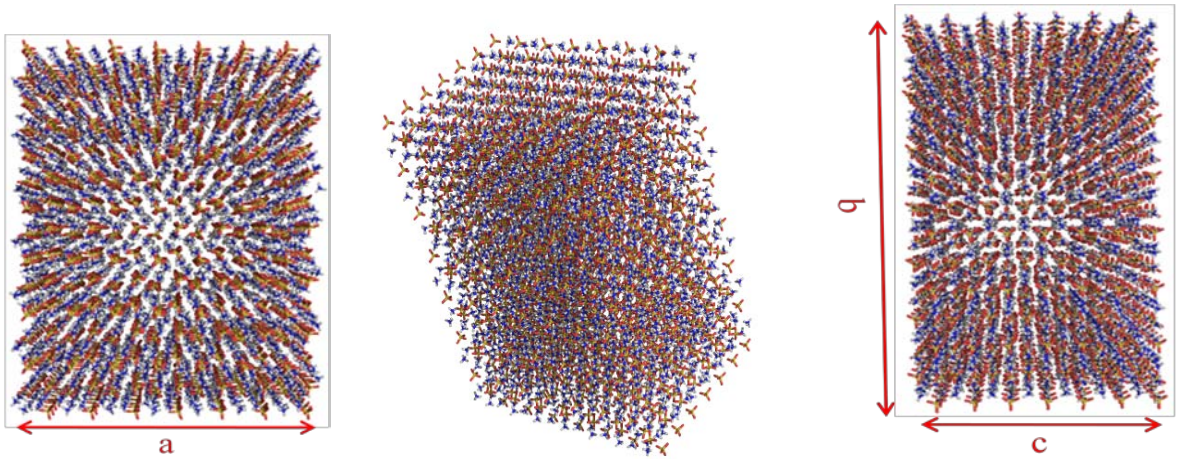

Figure 2. 5 Snapshots of a) 2m and b) 4m $(NH_4)_2SO_4$ aqueous solution without water molecules. S(yellow), O(red), N(blue), H(white)

a) **b)**

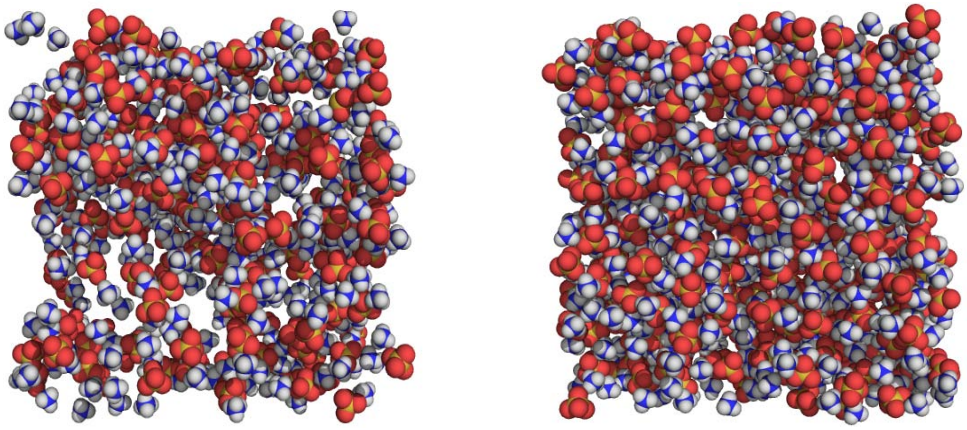

Figure 2. 6 Radial distribution functions obtained from the 2M simulation of $(NH_4)_2SO_4$. g_{cc}(black line), g_{ww}(red line), g_{cw}(green line)

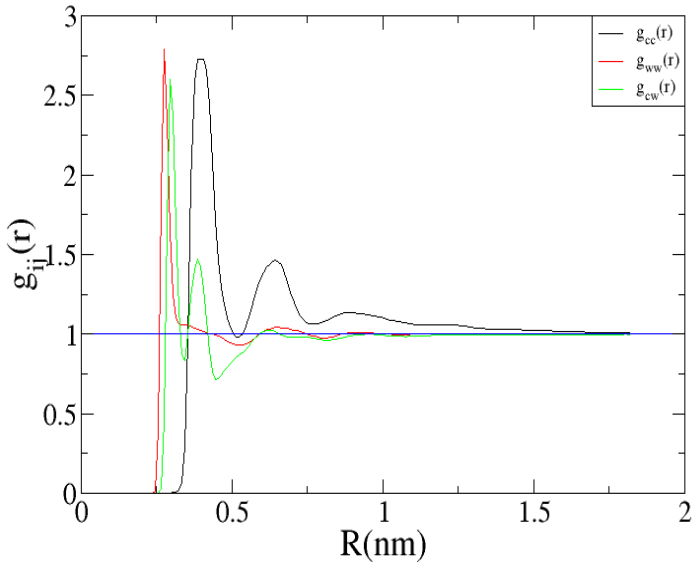

Figure 2. 7 Radial distribution functions of $(NH_4)_2SO_4$ between cosolvents obtained from the 2M simulation using different system sizes with box lengths of 6 - 24 nm.

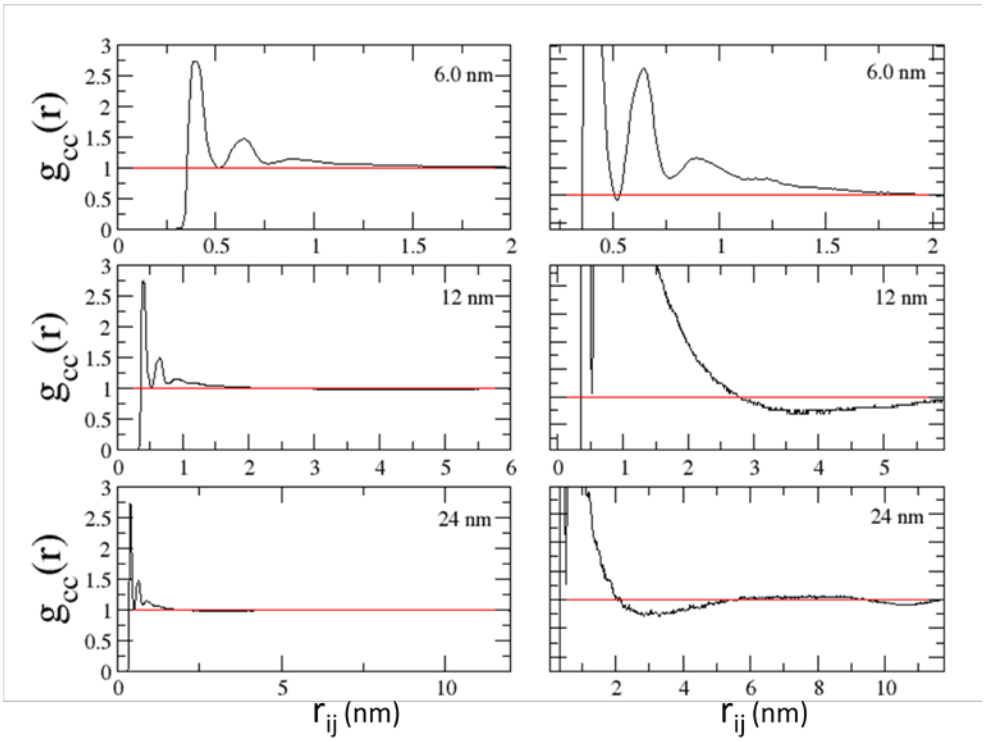

Figure 2. 8 Center of mass radial distribution functions (rdfs) as a function of distance (nm) and concentration for $(NH_4)_2SO_4$, Na_2SO_4, $NaClO_4$, $NaNO_3$.

a) $(NH_4)_2SO_4$

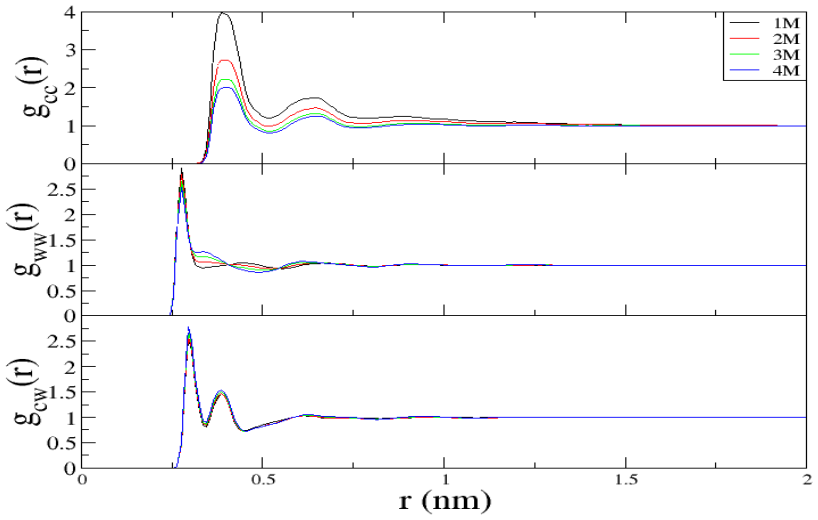

b) Na_2SO_4

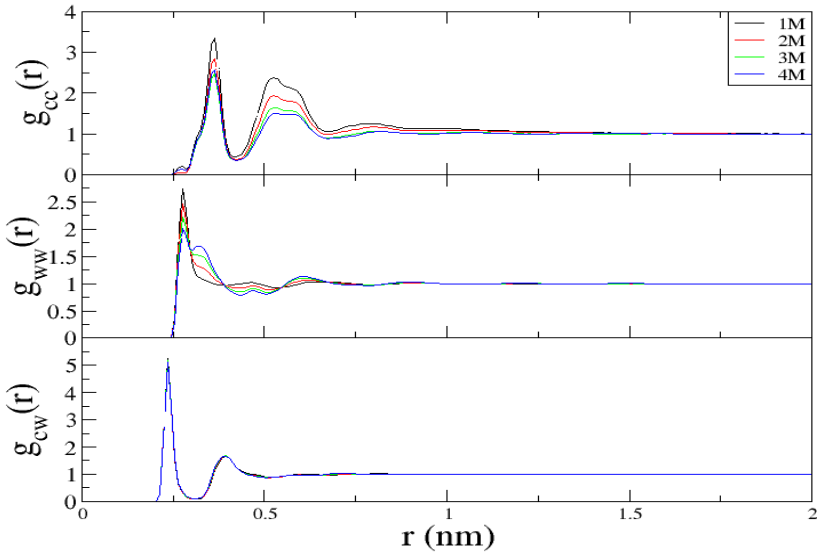

c) $NaClO_4$

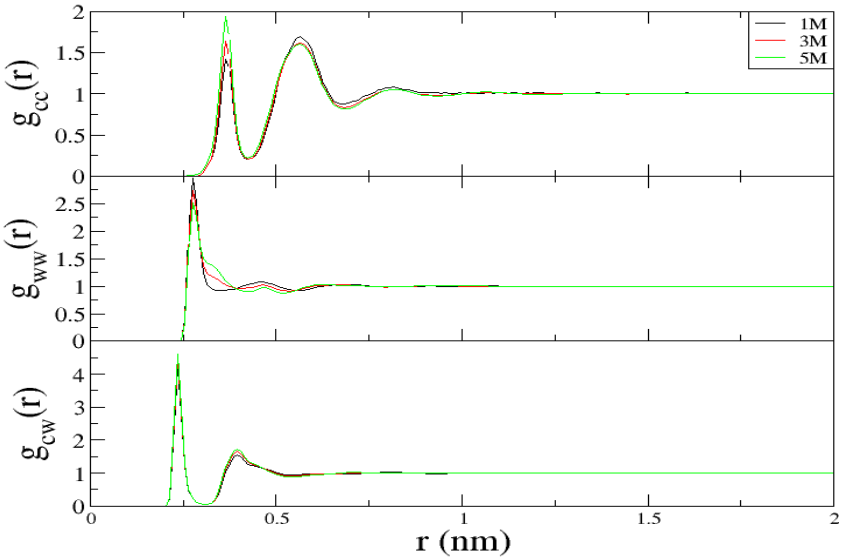

d) $NaNO_3$

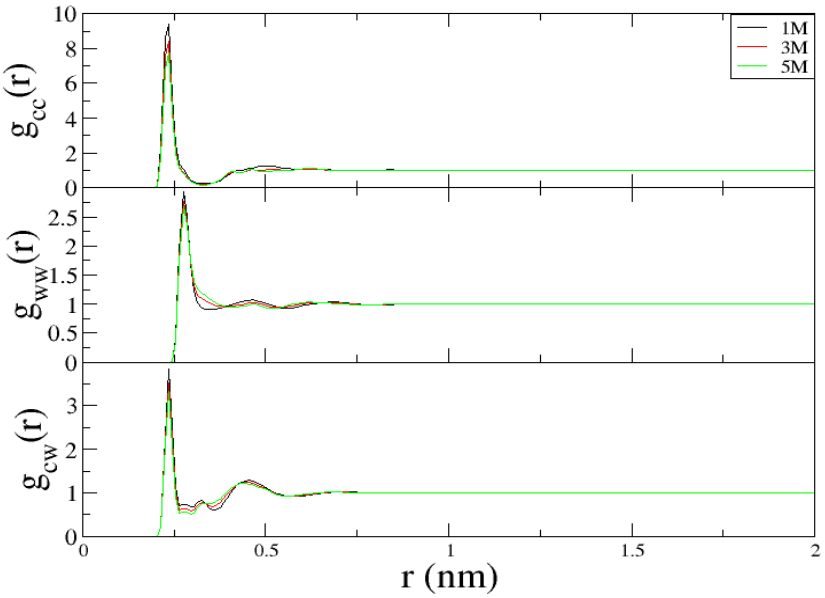

The center of mass radial distribution functions (rdfs) as a function of distance (nm) and concentration are displayed in Figure 2.8**.** Even at different concentrations, the positions of maxima and minima were mostly unaffected. The rdfs indicated that g_{cw} was essentially identical

for all four salts, while g_{cc} and g_{ww} were quite concentration dependent. This is especially true for g_{cc} of $(NH_4)_2SO_4$ and Na_2SO_4, where the first maximum and first minimum both increased with concentration.

Additionally, radial distribution functions for specific ion-ion and ion-water interactions are displayed in Figure 2.9. The corresponding first shell coordination numbers as a function of concentration are presented in Table 2.7, and exhibit the expected variation with concentration. The coordination numbers are defined by integration of the corresponding rdf to R_{min}. For $(NH_4)_2SO_4$ there was a very strong cation-anion contact pair probability which was somewhat concentration dependent. The first peak and the second peak in the rdf decreased with salt concentration. However no significant degree of solvent separated cation-anion pairing was evident, because the cation-water and anion-water rdf displayed a strong first peak as well. The solvation of both ions involved a large first peak in the ion to water oxygen rdfs. The peaks were positioned at 0.294 and 0.388 nm for the nitrogen and sulfur ions, respectively. The first peak in the water-water rdf decreased with salt concentration suggesting an decrease in water structure, and subsequent peaks displayed the same trend. The broadening of the first peak, like the shoulder, as a result of the reduction of the distance to the second solvation shell, was probably caused by ion effect. In Na_2SO_4 solutions the high solvation of both ions was evident in a large first peak in the ion to water oxygen rdfs. The peak positions for the sodium and sulfur ions were 0.23 and 0.387 nm, respectively. The first solvation peak for sodium was relatively high. The sodium to sulfur rdf displayed a large first and a significant second peak, which were obviously concentration dependent, and the peaks decreased with salt concentration. The first peak was of similar height of the second one, indicating indirect ion pairing between the anion and cation by water. This strong second peak suggests that the water did not separate the cation-anion pairing

significantly, even though both sodium and sulfate solvation peaks are large. The separation of sodium and water oxygen is smaller than sulfur and water oxygen because the positively charged sodium ion was directly attracted to the water oxygen, but sulfur was surrounded by four oxygens in sulfate decreasing the probability of water getting closer with water hydrogens oriented toward the anions. For all four salts, the separation between anions and water was always larger than the one between cation and water. A strong cation-anion contact pair probability was observed for $NaClO_4$. The first solvation peak for sodium was relatively high and located at 0.229 nm, while the peak for chloride was at 0.396 nm. In $NaNO_3$ solutions with increase in concentration, the +/- peak height was large and sharp due to the formation of contact ion pairs in the solution. The second peak could be assigned to the solvent-separated ion pairs formed in solution. The first solvation peak for the anion was relatively small, and the shoulder was very obvious and concentration dependent. The increase in concentration leads to a slight decrease of coordination numbers of water around the nitrate ions from 5.6 to 5.1. No peak showed significantly concentration dependent. The first peak for cation-water and water-water was 0.228, and 0.275 nm (See Table 2.7), compared to the X-ray diffraction experimental data, 0.244, 0.28nm, respectively.[47] Examining the cation-water rdfs, a slight decrease of the first peak could be observed with increasing concentration, due to the decrease in the coordination number from 5.1 to 3.9. The broad peak around 0.4 to 0.5 nm corresponded to the second hydration sphere of the sodium ion. The water-water peak decreases with increasing concentration and simultaneously becomes broader. A shoulder was caused by the contribution from the first hydration sphere of the ions. This effect clearly indicated the loss of the tetrahedral coordination of water in the second hydration sphere of the water in all solutions.

Figure 2. 9 Radial distribution functions obtained from simulation. Centers of cations, anions, and the water oxygens are denoted by the symbol +, -, and o, respectively. a) $(NH_4)_2SO_4$, 1M(black), 2M(red), 3M(green), 4M(blue) simulations. Cations (ammonium nitrogen), anions (sulfur); b) Na_2SO_4, 1M(black), 2M(red), 3M(green), 4M(blue) simulations. Cations (sodium), anions (sulfur); c) $NaClO_4$, 1M(black), 3M(red), 5M(green) simulations. Cations (sodium), anions (chloride); d) $NaNO_3$, 1M (black), 3M (red), 5M (green) simulations. Cations (sodium), anions (nitrogen).

a) $(NH_4)_2SO_4$

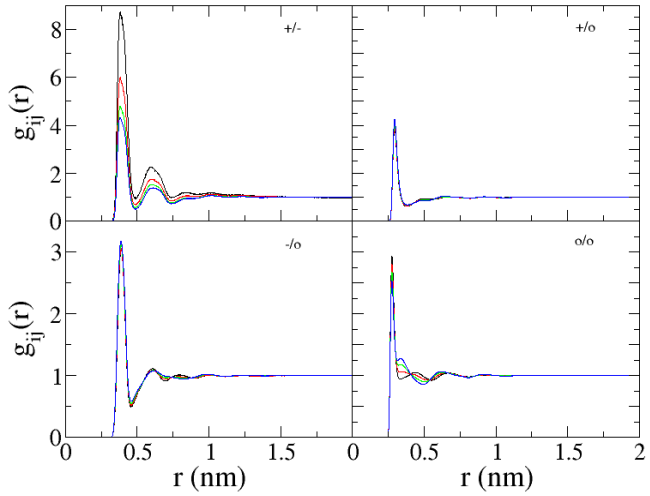

b) Na_2SO_4

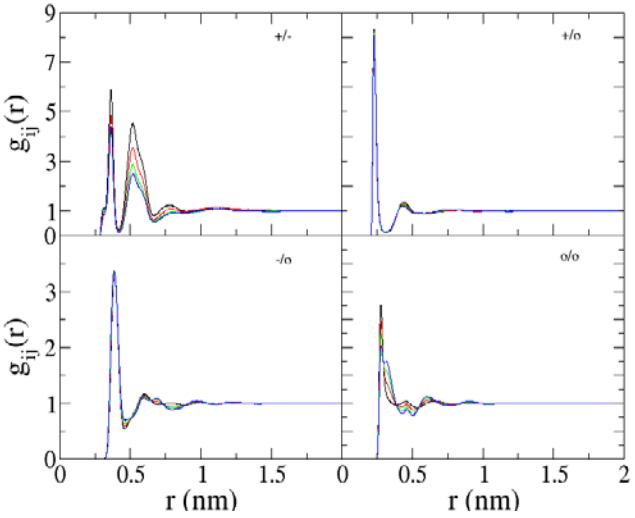

c) $NaClO_4$

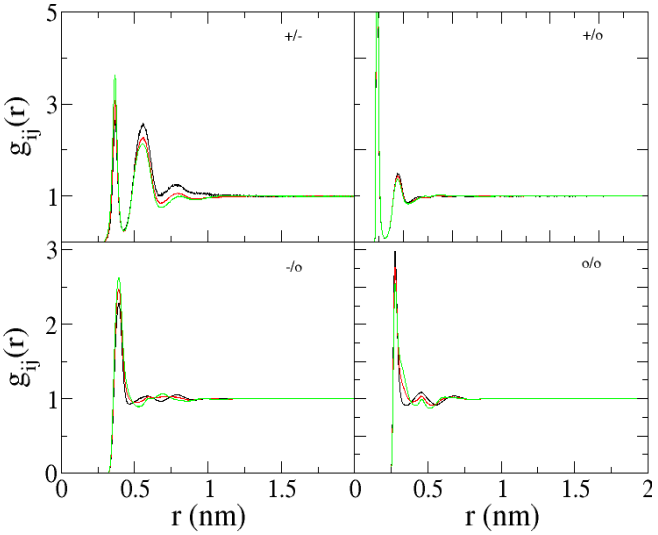

d) $NaNO_3$

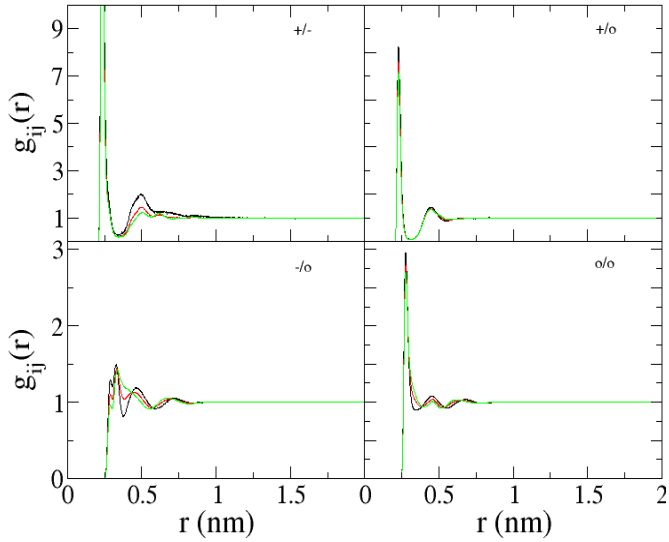

Figure 2. 10 Snapshots of the first solvation shell of (a) Na^+ (blue) and (b) SO_4^{2-} at 4M Na_2SO_4 solution. H_w(white), O_w(red), S(blue), O_s(yellow).

a) **b)**

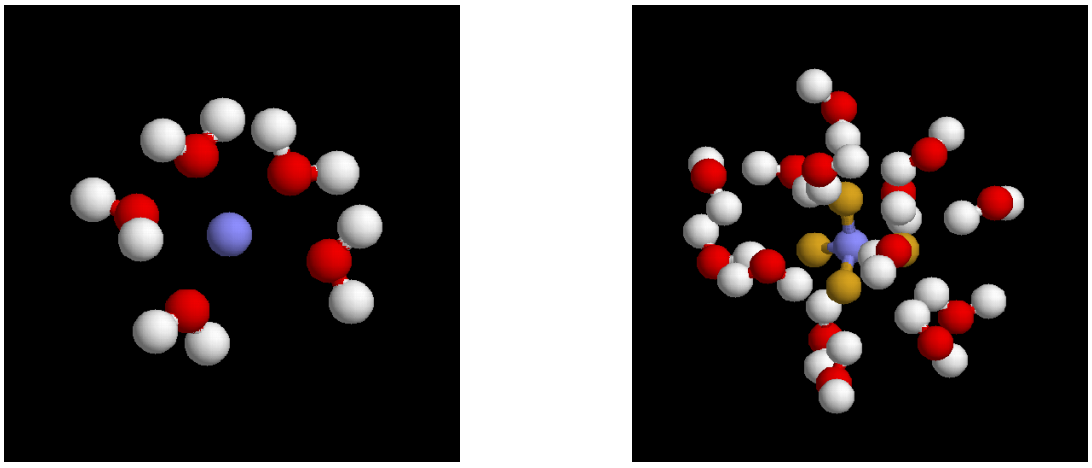

Figure 2. 11 Snapshots of the coordination shell around one bulk NO_3^- ion in 5M $NaNO_3$ The solvation shell (a) with waters less than 0.35 nm from the nitrate and (b) with waters belonging to the shoulder. H_W(white), O_W(red), N(blue), O_N(yellow)

a) **b)**

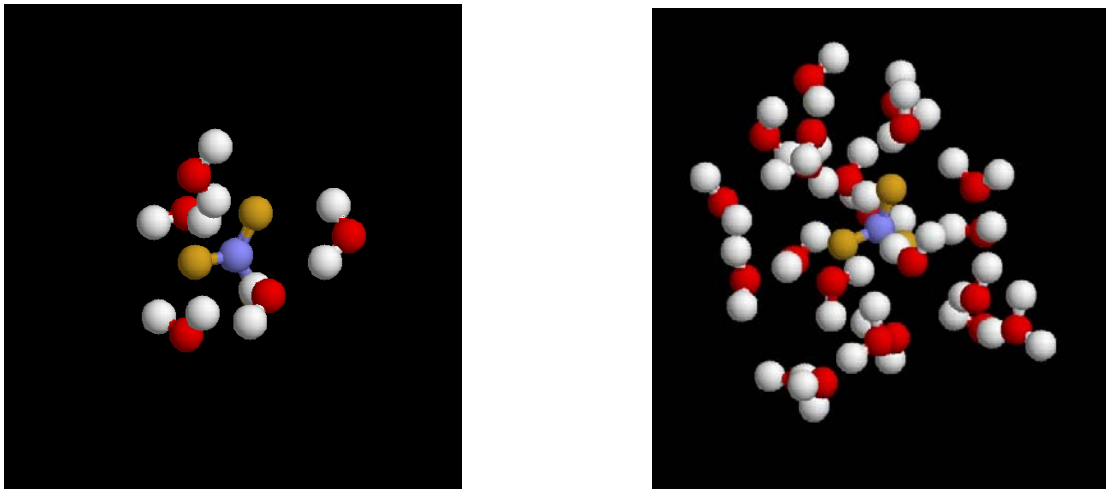

Table 2. 7 First shell coordination numbers for aqueous solutions. R_{max} and R_{min} are the positions (nm) of the first maximum and minimum in the rdf, respectively.

	m_s	+/-	+/o	-/o	o/o

$(NH_4)_2SO_4$	R_{max}		0.383	0.294	0.388	0.274
	R_{min}		0.488	0.378	0.455	0.331
	n_{ij}	1	0.812	7.313	12.26	4.130
		2	1.065	7.313	12.26	3.919
		3	1.219	6.958	11.62	3.697
		4	1.388	6.778	11.33	3.466
Na_2SO_4	R_{max}		0.364	0.23	0.387	0.276
	R_{min}		0.42	0.31	0.464	0.380
	n_{ij}	1	0.271	5.393	14.29	6.963
		2	0.848	5.282	14.28	7.166
		3	1.115	5.16	14.24	7.282
		4	1.487	4.976	14.12	7.252
$NaClO_4$	R_{max}		0.366	0.229	0.396	0.276
	R_{min}		0.427	0.313	0.470	0.349
	n_{ij}	1	0.115	5.508	11.88	4.982
		3	0.358	5.311	12.07	4.863
		5	0.652	5.063	12.09	4.705
$NaNO_3$	R_{max}		0.232	0.228	0.33	0.275
	R_{min}		0.346	0.312	0.38	0.346
	n_{ij}	1	0.280	5.120	5.617	4.951
		3	0.695	4.423	5.368	4.866
		5	0.652	3.910	5.106	4.716

As mentioned before, the thermodynamic properties of solution can be expressed in terms of the KB integrals. The KB integrals as a function of integration distance are displayed in

Figure 2.12. The KB integrals should reach a plateau value at the distance that the rdfs approached unity. The final KB integrals are typically averaged between 1.5 and 2 nm.

Figure 2. 12 Kirkwood-Buff integrals (cm^3/mol) as a function of integration distance (R) obtained from a) 4M $(NH_4)_2SO_4$, b) 4M Na_2SO_4, c) 5M $NaClO_4$, d) 5M $NaNO_3$, The black horizontal lines correspond to the values after averaging G_{ij}(R) between 1.5 and 2 nm.

a) $(NH_4)_2SO_4$

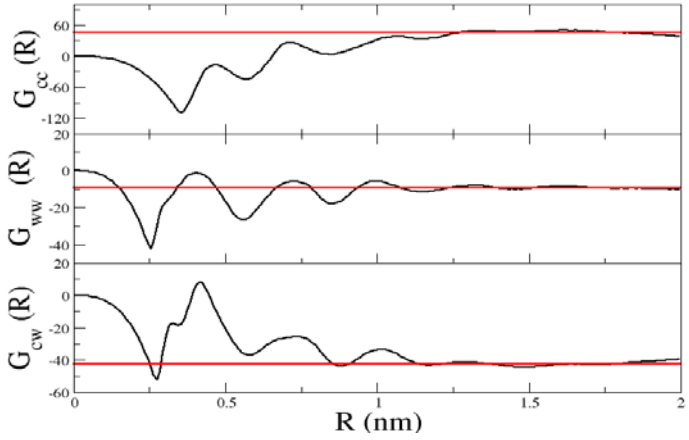

b) Na_2SO_4

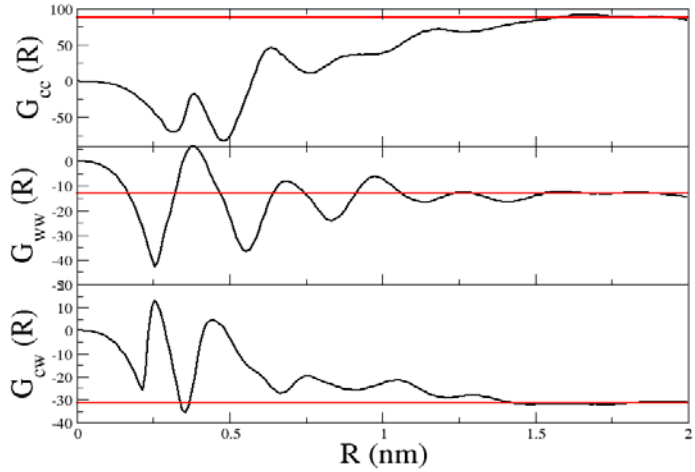

c) $NaClO_4$

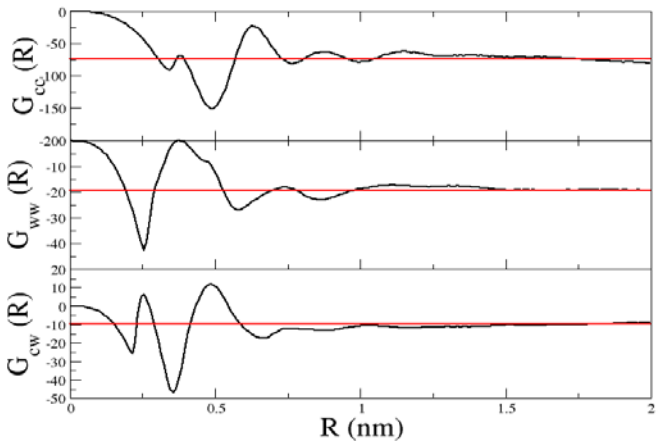

d) $NaNO_3$

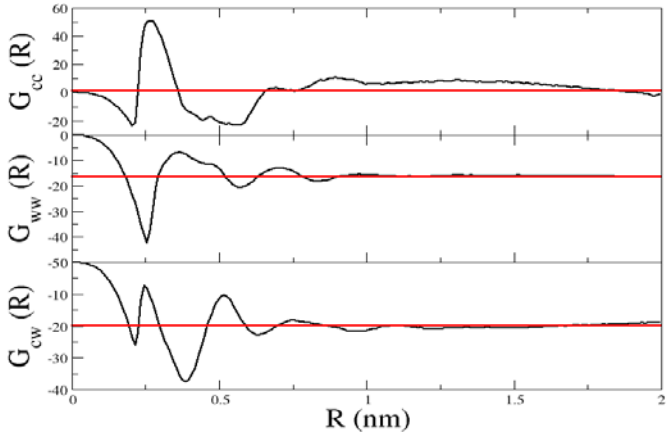

The excess coordination numbers obtained from the simulations are compared to the experimental data in Figure 2.13. Excess coordination numbers are used to suppress the inherent uncertainties by the equation $N_{ij} = \rho_j G_{ij}$, where G_{ij} at low concentrations can display significant uncertainty in the simulation and experimental data due to the relatively small number of ions present. For $(NH_4)_2SO_4$ and Na_2SO_4 solutions, the KBFF model reproduced desirable results except for low concentrations. There was a obvious overestimation in the self interactions (N_{cc} and N_{ww}) leading to a corresponding underestimation in N_{cw}. The experimental data was reproduced for all $NaClO_4$ and $NaNO_3$ concentrations.

Figure 2. 13 Excess coordination numbers as a function of concentration. The red lines correspond to the experimental data, the green cross to the raw simulation data. a) $(NH_4)_2SO_4$, b) Na_2SO_4, c) $NaClO_4$, d) $NaNO_3$.

a) $(NH_4)_2SO_4$

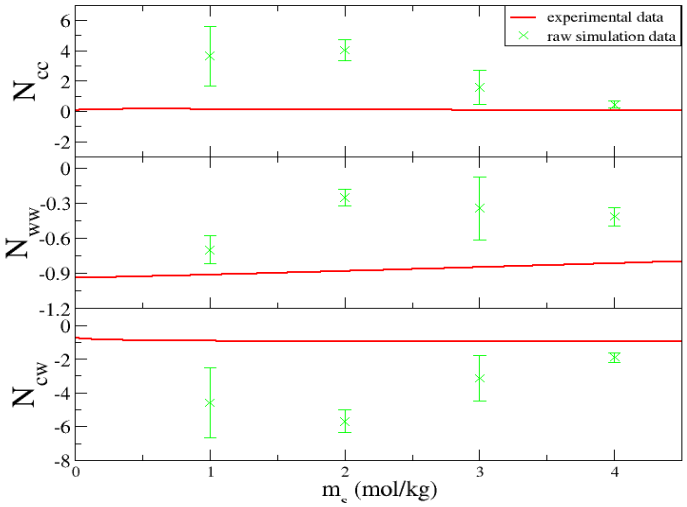

b) Na_2SO_4

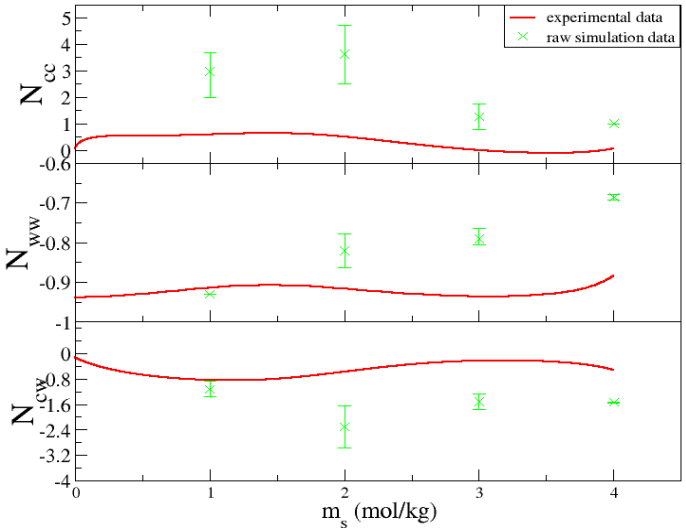

c) $NaClO_4$

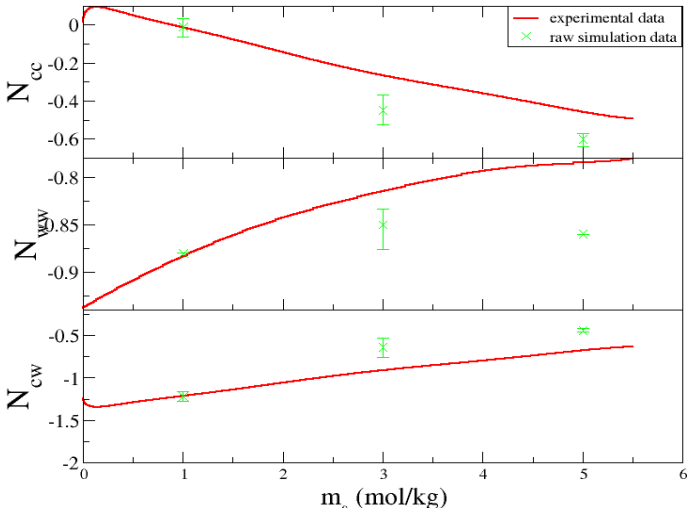

d) $NaNO_3$

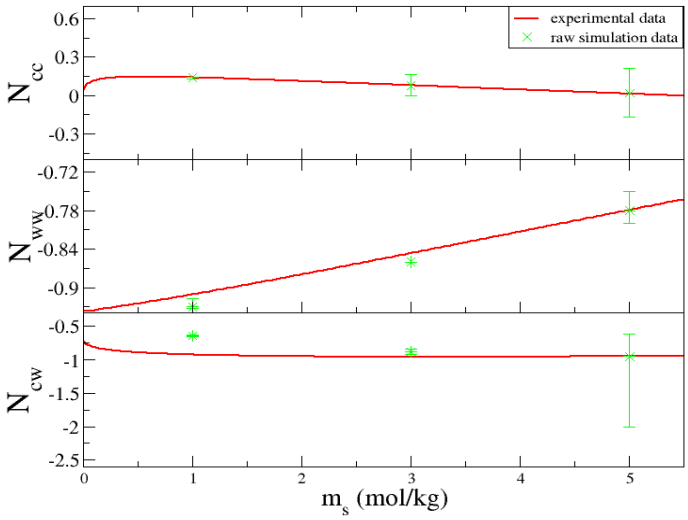

The experimental and simulated density and partial molar volumes are compared in Figure 2.14. The density was well reproduced. Salt and water partial molar volumes are compromising each other, when one is increasing, the other is decreasing. The activity derivative and relative permittivity are displayed in Figure 2.15. For $(NH_4)_2SO_4$ and Na_2SO_4 solutions, activity derivatives are always underestimated while $NaClO_4$ are overestimated. The relative

permittivity displayed the expected trend of a decrease with increasing concentration, but the experimental data could not be found.

Figure 2. 14 Solution density (g/cm^3) and partial molar volumes (cm^3/mol) as a function of concentration. Black lines correspond to the experimental data[48] and red crosses represent raw simulation data. a) $(NH_4)_2SO_4$, b) Na_2SO_4, c) $NaClO_4$, d) $NaNO_3$.

a) $(NH_4)_2SO_4$

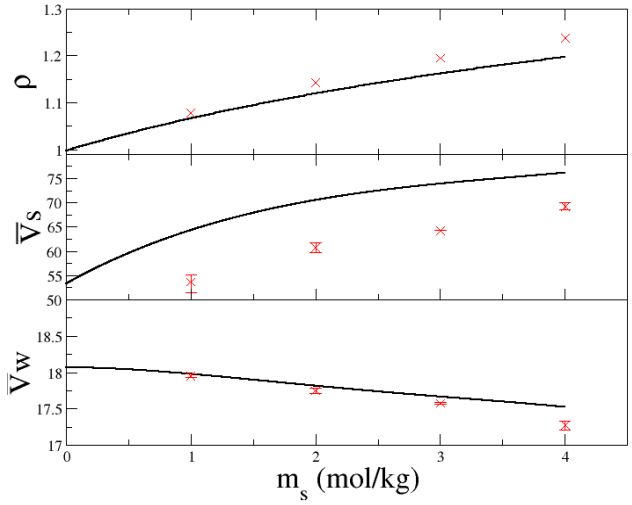

b) Na_2SO_4

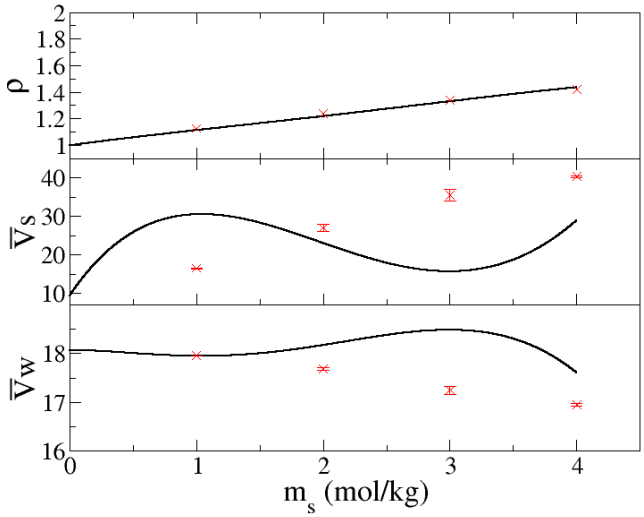

c) $NaClO_4$

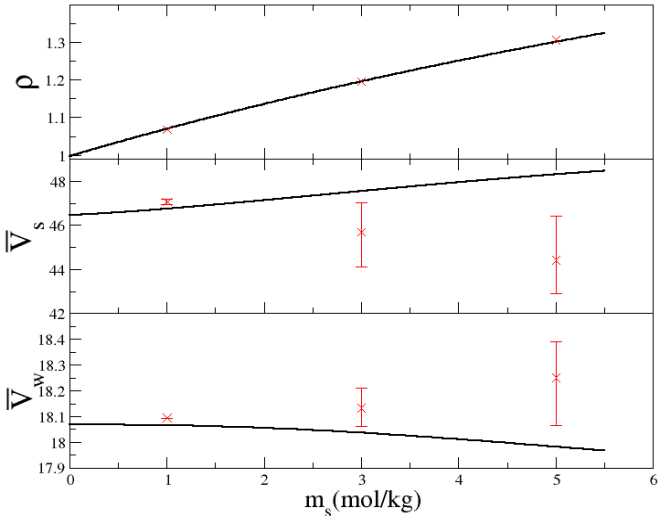

d) $NaNO_3$

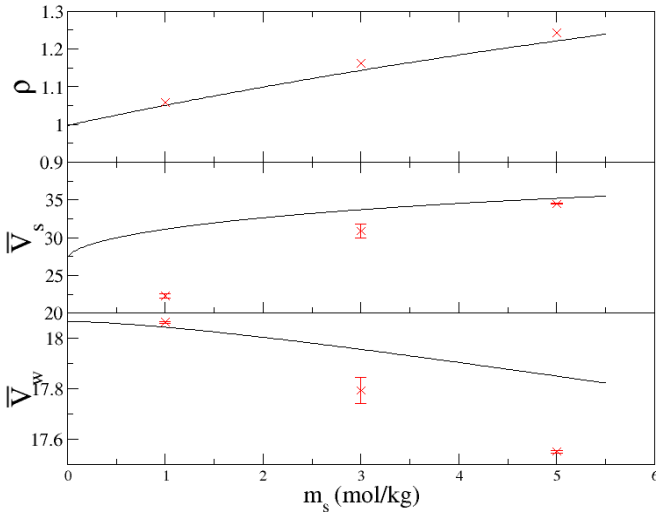

Figure 2. 15 Activity derivative[49,50] and relative permittivity as a function of concentration. Black lines represent the experimental data and red crosses correspond to the KBFF model. a) $(NH_4)_2SO_4$, b) Na_2SO_4, c) $NaClO_4$, d) $NaNO_3$.

a) $(NH_4)_2SO_4$

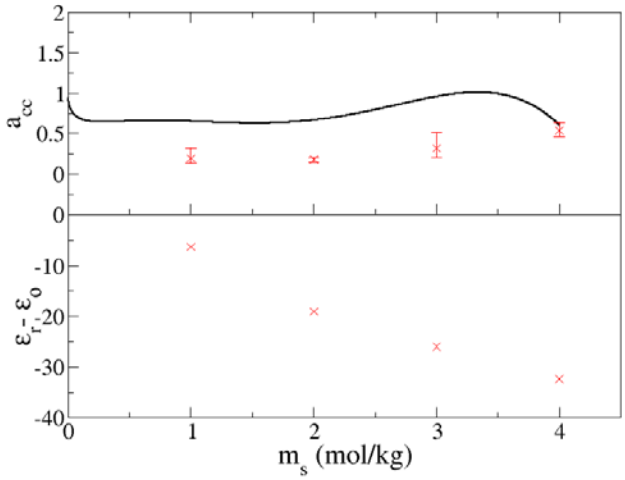

b) Na_2SO_4

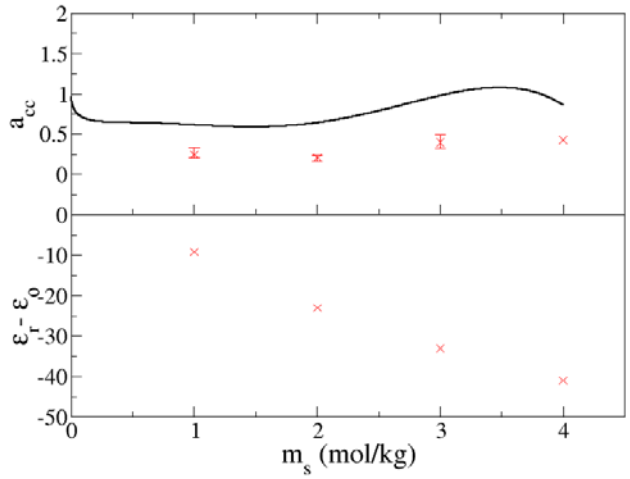

c) $NaClO_4$

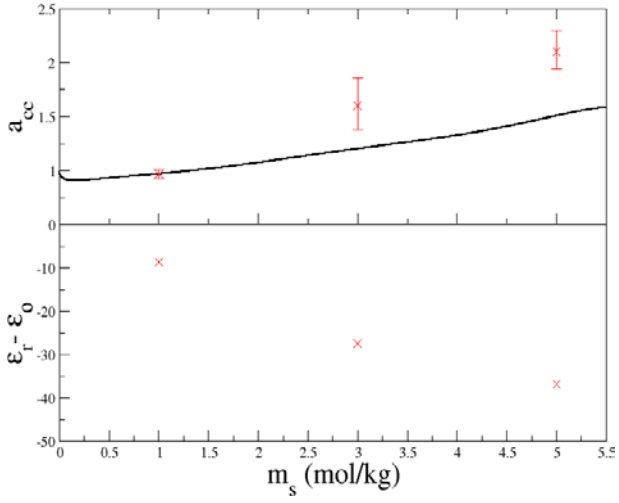

d) $NaNO_3$

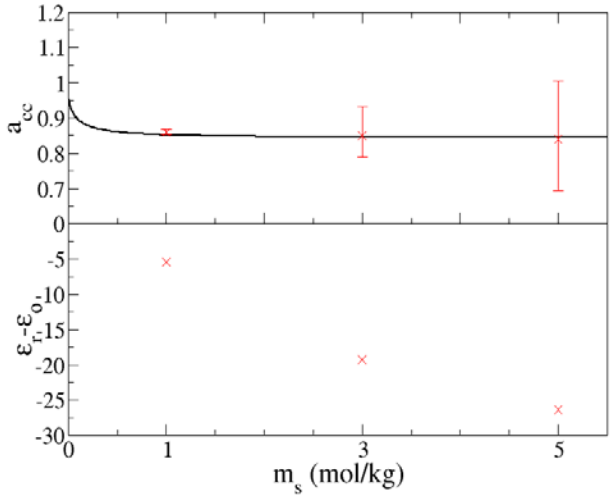

The cation, anion and water diffusion constants as a function of concentration are displayed in Figure 2.16. Unfortunately, some of the corresponding experimental values are unavailable. Our model reproduced well the available experimental trends, but slightly underestimated both ion diffusion constants.

Figure 2. 16 Diffusion constants ($10^{-9}m^2/s$) as a function of concentration. Lines represent the experimental data a) $(NH_4)_2SO_4$,[51-53] b) Na_2SO_4,[54,55] c) $NaClO_4$,[56] d) $NaNO_3$.

a) $(NH_4)_2SO_4$

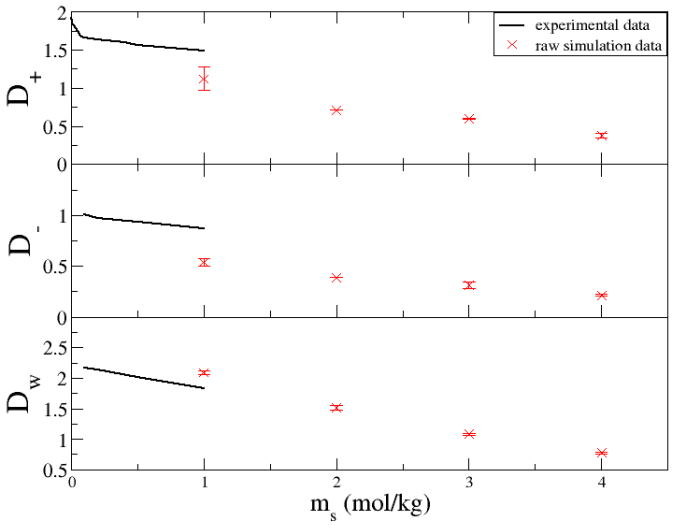

b) Na_2SO_4

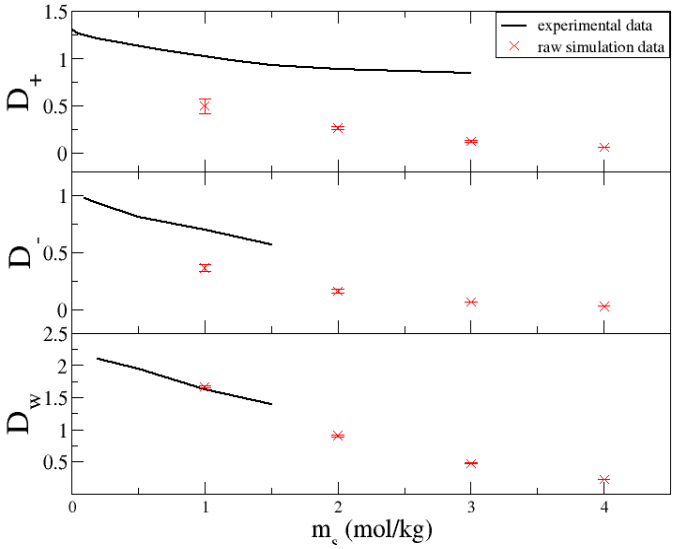

c) $NaClO_4$

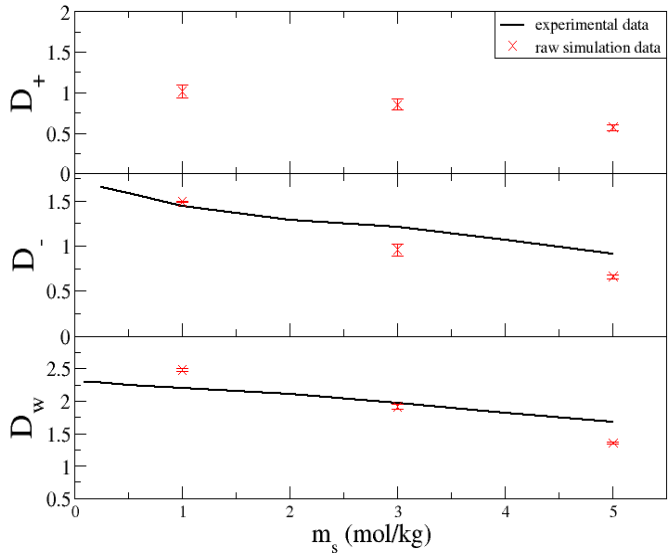

d) $NaNO_3$

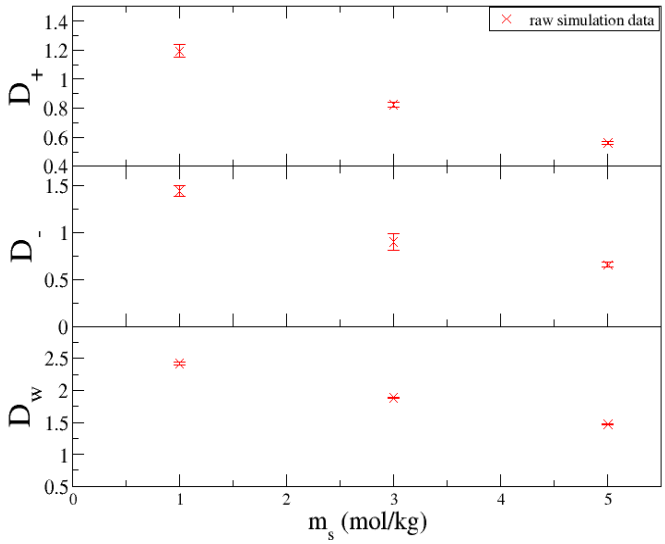

For Na_2CO_3 and Na_3PO_4 aqueous solutions, a wide variety of nonbonded parameters and even equilibrium bond lengths were investigated (see Table 2.8), but our models always displayed a high degree of self association at any concentration, which happened to $(NH_4)_2SO_4$ but only at low concentration. This is illustrated in Figure 2.17. An increase in the box size may provide a solution, but the simulations soon become computationally expensive. From the

Table 2. 8 range of bonded and nonbonded parameters studied for Na_3PO_4 and Na_2CO_3

Atom	q (e)	σ (nm)	ε (kJ/mol)	r_o [a] (nm)
P	-3～7	0.3～0.4	0.8368～1.046	1.53～1.58
O	-2.5～0	0.3～0.5	0.56～0.6047	
C	-2～4	0.31～0.377	0.33～0.417	1.27～1.29
O	-2～0	0.31～0.35	0.56～0.6047	

a. Equilibrium bond length

Figure 2. 17 Snapshot of (a) Na_2CO_3 (b) Na_3PO_4. aqueous solution without water molecules. For Na_2CO_3, Na(blue), C(gray), O(red); For Na_3PO_4, Na(blue), P(yellow), O(red).

a) **b)**

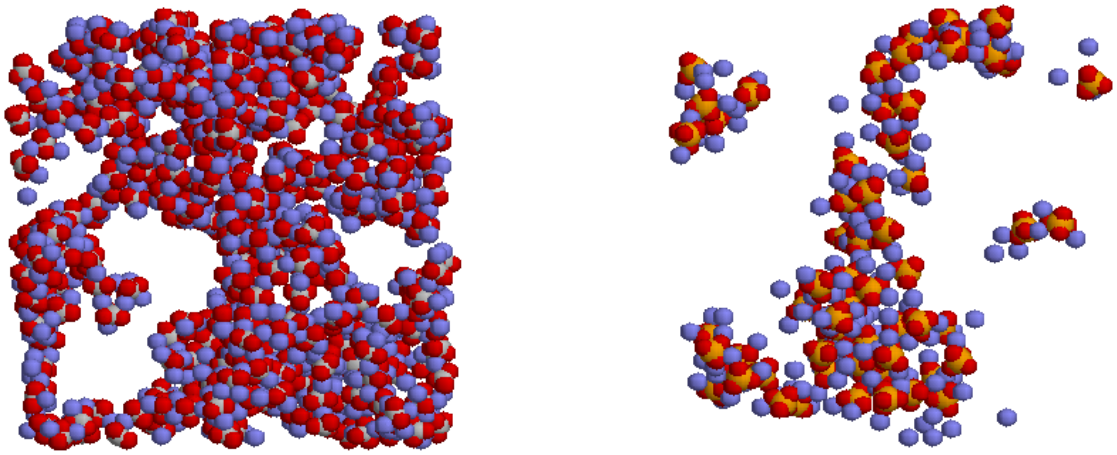

Table 2. 9 Comparison of the KBI and properties of 2M $(NH_4)_2SO_4$ and 0.5M Na_3PO_4 solution obtained with different treatment of cutoff.

$(NH_4)_2SO_4$	Nstlist (steps)	Rlist (nm)	rcoul (nm)	rvdw (nm)	G_{cc} (cm^3/mol)	G_{ww} (cm^3/mol)	G_{cw} (cm^3/mol)	ρ (g/cm^3)	a_{cc}
EXP					60	-14	-34	1.12	0.67
SIM	10	0.8	0.8	1.5	745	-5	-114	1.14	0.18
	10	1.0	1.0	1.5	923	-4	-130	1.14	0.15
	5	1.0	1.0	1.5	654	-8	-96	1.14	0.2
	10	1.5	1.5	1.5	425	-11	-71	1.14	0.27
	5	1.5	1.5	1.5	668	-7	-66	1.14	0.19

Na_3PO_4	nstlist (steps)	rlist (nm)	rcoul (nm)	rvdw (nm)	G_{cc} (cm^3/mol)	G_{ww} (cm^3/mol)	G_{cw} (cm^3/mol)	ρ (g/cm^3)	a_{cc}
EXP					724	-17	-1	1.08	0.41
SIM	10	0.8	0.8	1.5	9142	-16	84	1.09	0.05
	10	1.0	1.0	1.5	9715	-16	95	1.09	0.04
	5	10	10	1.5	10742	-16	109	1.09	0.04
	10	1.5	1.5	1.5	6741	-16	65	1.09	0.07
	5	1.5	1.5	1.5	11679	-16	108	1.09	0.04

nstlist: update frequency of neighbor list
rlist: cutoff distance for the short-range neighbor list
rcoul: cutoff distance for Coulomb interactions
rvdw: cutoff distance for van der Waals interactions

experimental pKa's,[57] we know that contributions from hydrolysis can become very large at low molalities for these two electrolytes, especially for Na_3PO_4. The high pKa's for CO_3^{2-} and PO_4^{3-} indicate that these are minority species in neutral aqueous solutions.[58] However, we do not know the pH at which the activities were determined. So the reliability of experimental data, and the exact species present in solutions, for these two systems are in some doubt. Alternatively, considering that SO_4^{2-} and CO_3^{2-} are bivalent anions and PO_4^{3-} is a trivalent anion, the electrostatic interactions are much stronger compared to ClO_4^- and NO_3^-. Hence, polarization effects will be large and may not be adequately modeled with a simple effective charge model. However, the reason for this disagreement is unknown. To investigate further, we decreased the nstlist parameters from 10 to 5 steps to increase the frequency of update of neighbor list, and increased rcoul from 0.8 to 1.0 and 1.5 nm to make the cut-off for Coulombic interactions larger. The results are presented in Table 2.9. We observed some improvement, but not sufficient.

2.4 Conclusions

KBFF models for $(NH_4)_2SO_4$, Na_2SO_4, $NaClO_4$, $NaNO_3$ have been developed which reproduce the experimental solution density and KB integrals as a function of salt concentration, as well as several other properties. Radial distribution functions and KB integrals assist us in studying the molecular level and bulk properties. The difference among KB integrals obtained from KBFF, Singh et al, Cannon et al models for $(NH_4)_2SO_4$ was significant. We were unable to developed a realistic model for Na_2CO_3 and Na_3PO_4 as yet. Both of these two salt solutions show a high degree of aggregation at any concentration, while this kind of deviation only happened to $(NH_4)_2SO_4$ and Na_2SO_4 at low concentration. An increase in the box size may solve this problem but is computationally expensive. Alternatively, changes to the parameters of

treatment of cutoffs can improve the simulation data somewhat bit but not enough. Kirkwood-Buff force fields are nonpolarizable which neglect the effect of induced-dipoles. Therefore, one of the reasons leading to these big deviations might be due to the fixed-dipole environment that is not accurately applied to the system like aqueous Na_2CO_3, Na_3PO_4 solutions due to their high charge density**.**

References

1. Leibler, L.; Pezron, E.; Pincus, P. A. (1988). Viscosity behavior of polymer solutions in the presence of complexing ions. Polymer, 29(6), 1105-1109.
2. Bostrom, M.; Williams, D. R. M.; Ninham, B. W. (2001). Surface tension of electrolytes: specific ion effects explained by dispersion forces. Langmuir, 17(15), 2275-4478.
3. Hribar, B.; Southall, N. T.; Vlachy, V.; Dill, K. A. (2002). How ions affect the structure of water. J. Am. Chem. Soc., 124(41), 12302-12311.
4. Ben-Naim, A.Hydrophobic interactions, Plenum Press, New York, 1980
5. Southall, N.T.; Dill, K.A.;Haymet,A.D.J.(2002). A view of hydrophobic effect. J.Phys,Chem.B,106(3),421-533
6. Holz, M.; Grunder, R.; Meleleo, A. (1993). Nuclear magnetic resonance study of self-association of small hydrophobic solutes in water: salt effects and the lyotropic series. J. Chem. Soc., Faraday Trans, 89, 1215-1222.
7. Westh, P.; Kato, H.; Nishikawa, K.; Koga, Y. (2006). Toward understanding the Hofmeister series. 3. Effects of sodium halides on the molecular organization of H_2O as probed by 1-propanol. J. Phys. A,110(5), 2072-2078
8. Zangi, R.; Hagen, M.; Berne, B.J. (2007). Effects of ions on the hydrophobic interaction between two plates. J. Am. Chem. Soc., 129(15), 4678-4686.
9. Kunz, W. (2006). Specific ion effects in liquids, in biological systems, and at interfaces. Pure Appl. Chem., 78(8), 1611-1617

10. Cacace, M. G.; Landau, E. M.; Ramsden, J. (1997). The Hofmeister series: salt and solvent effects on interfacial phenomena. Quat. Rev. Biophys., 30, 241-277.
11. Hofmeister, F. (1888). On the understanding of the effects of salts. Arch. Exp. Pathol. Pharmacol. 24, (1888) 247-260.
12. Howe. P. E. (1921). The use of sodium sulfate as the globulin precipitant in the determination of proteins in blood. J. Bio. Chem., 49, 93-107.
13. Urbansky, E. T.(1998). Perchlorate chemistry: implications for analysis and remediation. Bioremediation Journal, 2(2), 81-95.
14. Huang, X.; Evangelou, V. P. (1993). Suppression of pyrite oxidation rate by phosphate addition. Environmental Geochemistry of Sulfide Oxidation. Chapter 34, (pp. 562-573).
15. Voet, D.; Voet, J. (1995). Biochemistry, 2nd edn., (pp.428-434). J. Wiley & Sons Inc., New York,
16. Pribil, A. B.; Hofer, T. S.; Randolf, B. R.; Rode, B. M. (2008). Structure and Dynamics of Phosphate ion in aqueous solution: An Ab Initio QMCF MD Study. J. Comp. Chem., 29(14), 2330-2334.
17. Singh, U. C.; Brown, F. K.; Bash, P. A.; Kollman, P. A. (1987). An approach to the application of free energy perturbation methods using molecular dynamics: applications to the transformations of $CH_3OH \rightarrow CH_3CH_3$, $H_3O^+ \rightarrow NH_4^+$, glycine→alanine, and alanine→ phenylalanine in aqueous solution and to $H_3O^+(H_2O)_3 \rightarrow NH_4^+(H_2O)_3$ in the gas phaseJ. Am. Chem. Soc. 1987, 109(6), 1607-1614.
18. Cannon, W.R.; Pettitt, B. M.; McCammon, J. A. (1994). Sulfate Anion in Water: Model Structural, Thermodynamic, and Dynamic Properties. *J. Phys. Chem.*, 98 (24), 6225–6230.

19. Kirkwood, J. G.; Buff, F. P. (1951).The statistical mechanical theory of solutions. J. Chem. Phys., 19(6), 774-777.
20. Ben-Naim, A. (1977). Inversion of Kirkwood-Buff theory of solutions-application to water-ethanol system. J. Chem. Phys., 67(11), 4884-4890.
21. Ben-Naim, A. (1992). Statistaical thermodynamics for chemists and biochemists. Plenum Press, New York.
22. Kusalik, P. G.; Patey, G. N. (1987). The thermodynamic properties of electrolyte solutions: some formal results. J. Chem. Phys., 86(9), 5110-5117.
23. Friedman, H. L.; Ramanathan, P. S. (1970). Theory of mixed electrolyte solutions and application to a model for aqueous lithium chloride-cesium chloride. J. Phys. Chem., 74(21), 3756-3765.
24. Behera, R. (1998). On the calculation of thermodynamic properties of electrolyte solutions from Kirkwood-Buff theory. J. Chem. Phys., 108(8), 3373-3375.
25. Matteoli, E. (1997). A study on Kirkwood-Buff integrals and preferential salvation in mixtures with small deviations from ideality and/or with size mismatch of components. Importance of a proper reference system. J. Phys. Chem. B, 101(47), 9800-9810.
26. Berendsen, H. J. C.; Grigera, J. R.; Straatsma, T. P. (1987).The missing term in effective pair potentials. J. Phys. Chem., 91, 6269-6271.
27. Hess, B.; Kutzner, C.; van der Spoel, D.; Lindalhl, E. (2008). GROMACS 4: Algorithms for highly efficient, load-balanced, and scalable molecular simulation. Journal of Chemical Theory and Computation, 4(3), 435-447.
28. van der Spoel, D.; Lindahl, E.; Hess, E.; Groenhof, G.; Mark, A. E.; Berendsen, H. J. C. (2005). GROMACS: Fast, flexible, and free. J. Comp. Chem., 26(16), 1701-1718.

29. Lindahl, E.; Hess, B.; van der Spoel, D.; (2001). GROMACS 3.0: a package for molecular simulation and trajectory analysis. Journal of Molecular Modeling, 7(8), 306-317.

30. Berendsen, H. J. C.; Postma, J. P. M.; van Gunsteren, W. F.; Dinola, A.; Haak, J. R. (1984). Molecular-Dynamics with coupling to an external bath. J. Chem. Phys., 81(8), 3684-3690.

31. Ryckaert, J. P.; Ciccotti, G.; Berendsen, H. J. C. (1977). Numerical integration of the Cartesian equations of motion of a system with constraints: molecular dynamics of n-alkanes. J. Comp. Phys., 23(3), 327-341.

32. Sugita, Y. O. Y. (1999). Replica-exchange molecular dynamics method for protein folding. Chemical Physics Letter, 314(12), 141-151.

33. Darden, T.; York, D; Pedersen, L.; (1993). Particle Mesh Ewald – An N. Log(N) method of Ewald sums in large systems. J. Chem. Phys., 98(12), 10089-10092.

34. Chitra, R.; Smith, P. E. (2000). Molecular dynamics simulations of the properties of cosolvents solutions. J. Phys. Chem. B, 104(24), 5854-5864.

35. Allen, M. P.; Tildesley, D. J. (1987). Computer Simulation of liquids. Oxford University Press, Oxford.

36. W. F. van Gunsteren, S. R. Billeter, A. A. Eising, P. H. Hunenberger, P. Kruger, A. E. Mark, W. R. P. Scott, and I. G. Tironi. (1996). Biomolecular Simulation: The GROMOS96 Manual and User Guide. vdf hochschulverlang, ETH zurich, Switzerland.

37. Daura, X.; Mark, A. E.; van Gunsteren, W. F. (1998). Parametriztion of aliphatic CHn united atoms of GROMOS96 force field. Journal of Computational Chemistry, 19(5), 535-547.

38. de Boer, J. L.; Vos, A. (1971).The crystal structure of the room- and low- temperature modifications of Wurster's blue perchlorate, TMPD.ClO_4. I. The room-temperature phase. Acta. Cryst., B28, 835-839.

39. Kraut, J.; Jensen, L. H. (1963). Refinement of the crystal structure of adenosine-5'-phosphate. Acta. Cryst., 16, 79-88.

40. Thomas, J. L.; Roeselova, M.; Dang, L. X.; Tobias, D. J. (2007). Molecular dynamics simulations of the solution-air interface of aqueous sodium nitrate. J. Phys. Chem. A, 111, 3091-3098.

41. Betzel, C.; Saenger, W.; Loewus, D. (1982). Sodium Carbonate Heptahydrate. Acta Cryst.,B38, 2802-2804.

42. Weerasinghe, S.; Smith, P. E. (2003). A Kirkwood-Buff derived force field for sodium chloride in water. J. Chem. Phys., 112(21), 11342-11349.

43. Weerasinghe, S.; Smith, P. E. (2004). A Kirkwood-Buff derived force field for the simulation of aqueous guanidinium chloride solutions. J. Chem. Phys., 121(5), 2180-2186.

44. Weerasinghe, S.; Smith, P. E.(2003). Kirkwood-Buff derived force field for mixtures of acetone and water. J. Chem. Phys., 118(23), 10663-10671.

45. Schlemper, E. O.; Hamilton, W. C. (1966). Neutron-diffraction study of the structures of ferroelectric and paraelectric ammonium sulfate. The Journal of Chemical Physics, 44(12),4498-4509.

46. Georgalis, Y.; Kierzek, A. M.; Saenger, W. (2000). Cluster formation in aqueous electrolyte solutions observed by dynamic light scattering. J. Phys. Chem. B, 104, 3405-3406.

47. Megyes, T.; Balint, S. (2009). Solution structure of $NaNO_3$ in water: diffraction and molecular dynamics simulation study. J. Phy. Chem B, 113, 4054-404.

48. Sohnel, O.; Novotny, P. (1985). Physical sciences data22, densities of aqueous solutions of inorganic substances. Elsevier.

49. El Guendouzi, M.; Mounir, A.; Dinane, A. (2003). Water activity, osmotic and activity coefficients of aqueous solutions of Li_2SO_4, Na_2SO_4, K_2SO_4, $(NH_4)_2SO_4$, $MgSO_4$, $MnSO_4$, $NiSO_4$, $CuSO_4$, and $ZnSO_4$ at T=298.15K. Journal of Chemical Thermodynamics, 35(2), 209-220.

50. Robinson, R. A.; Stokes, R. H. (1949). Tables of osmotic and activity coefficients of electrolytes in aqueous solution at 25 ℃. Imperial Chemical Industries Fellow, University of Cambridge.

51. Tanaka, K; Hashitani,T.(1971). Measurements of self-diffusion coefficients of ammonium ion in aqueous solutions. Trans. Faraday Soc.**,** 67**,** 2314 – 2317.

52. Tanaka, K. (1988). Measurements of tracer diffusion coefficients of sulphate ions in aqueous solutions of ammonium sulphate and sodium sulphate, and of water in aqueous sodium sulphate solutions. J.chem. Soc., Faraday Trans. 1, 84(8), 2895-2897

53. Tanaka, K.(1975). Measurements of self-diffusion coefficients of water in pure water and in aqueous electrolyte solutions. J. Chem. Soc., Faraday Trans. 1**,** 71, 1127 – 1131.

54. Tanaka, K. (1988). Measurements of tracer diffusion coefficients of sulphate ions in aqueous solutions of ammonium sulphate and sodium sulphate, and of water in aqueous sodium sulphate solutions. J.chem. Soc., Faraday Trans. 1, 84(8), 2895-2897

55. Nielsen, J. M.; Adamson, A. W.; Cobble, J. W. (1952).The self-diffusion coefficients of the ions in aqueous sodium chloride and sodium sulfate at 25 ℃. *J. Am. Chem. Soc.,74* (2), 446–451

56. Hell, S.T.; Holz, M.; Kastner, T. M.; Weingrtner, H. J. (1993). Self-diffusion of the perchlrate ion in aqueous electrolyte solutions measured by ^{35}Cl NMR spin-echo experiments. Chem. Soc., Faraday Trans, 91(12), 1877-1880.

57. Maegawa, T.; Kitamura, Y.; Sako, S. (2007). Heterogeneous Pd/C-catalyzed ligand-free, room-temperature Suzuki-Miyaura coupling reactions in aqueous Media. Chem. Eur. J., 13(20), 5937-5943.

58. Vanderzee, C. E. (1982). Thermodynamic properties of solutions of a hydrolyzing electrolyte: relative partial molar enthalpies and heat capacities, solvent activities, osmotic coefficients, and solute activity coefficient of aqueous sodium carbonate. J. Chem. Thermodynamics, 14, 1051-1067.

59. Pye, C. C.; Rudolph, W. W. (2003). An ab initio, infrared, and Raman investigation of phosphate ion hydration. J. Phys. Chem. A, 107, 8746-8755.

CHAPTER 3 - Summary and Future Work

The powerful technique of MD simulation provides an indispensible approach for the study of the system of interest at atomic level. Kirkwood-Buff (KB) theory, arguably the most important one in solutions relating molecular distributions to thermodynamic properties, plays an important role in characterizing the ion-ion, ion-water, water-water interactions in aqueous solution. MD simulation and KB theory are combined together and applied to study a variety of systems. Here, this combination is demonstrated well for ammonium sulfate, sodium sulfate, sodium perchlorate and sodium nitrate aqueous solutions. The results we have suggest that the KBFF models developed by Dr. Smith and his colleagues are very promising and competitive compared to other existing force fields. We found that the current KBFF could not reproduce KB integrals for sodium carbonate and sodium phosphate. Therefore, in our future work, we will continue to improve the KBFF models in order to provide more accurate microscopic detail and macroscopic properties on the study of the system of interest.